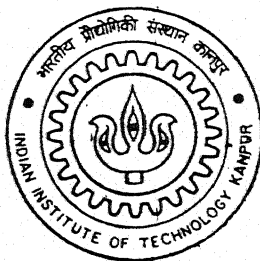


A KNOWLEDGE BASED PROCESS PLANNING SYSTEM FOR AXISYMMETRIC DEEP DRAWING

By

AJIT KUMAR SAHU



TH
ME/2002/M
Sa 19k

DEPARTMENT OF MECHANICAL ENGINEERING

Indian Institute of Technology Kanpur

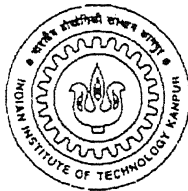
FEBRUARY, 2002

A KNOWLEDGE BASED PROCESS PLANNING SYSTEM FOR AXISYMMETRIC DEEP DRAWING

A Thesis Submitted
In Partial Fulfilment of the Requirements
for the Degree of
Master of Technology

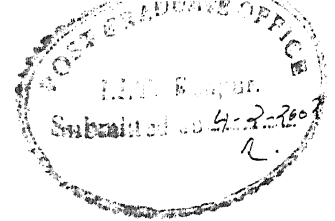
by

AJIT KUMAR SAHU

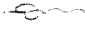



to the
DEPARTMENT OF MECHANICAL ENGINEERING
INDIAN INSTITUTE OF TECHNOLOGY KANPUR
FEBRUARY, 2002

CERTIFICATE



It is certified that the work contained in the thesis entitled "*A Knowledge based process planning system for axisymmetric deep drawing*", by *Mr. Ajit Kumar Sahu*, has been carried out under our supervision and that this work has not been submitted elsewhere for a degree.


Dr. P.M. Dixit
Dept. of Mechanical Engineering and
I.I.T Kanpur


Dr. N.V.Reddy
Dept. of Mechanical Engineering
I.I.T. Kanpur

FEBRUARY, 2002

- 5 MAR 2002/ME

पुरुषोत्तम लाल शर्मा केंद्र पुस्तकालय
भारतीय प्रौद्योगिकी संस्थान कानपुर
अवाप्ति क्र० A....137933.....

It is
cess p
has be
where

D
D
I

R



A137933

Acknowledgements

I express my sincere gratitude, regards and thanks to my supervisors Prof. N. V. Reddy and Prof. P.M. Dixit for their excellent guidance, invaluable suggestions and generous help at all the stages of my research work. Their interest and confidence in me was the reason for all the success I have made.

I would like to thank to my classmates for their smile and friendship making the life at I.I.T. Kanpur enjoyable and memorable.

I gratefully acknowledge the financial assistance from Department of Science and Technology, India for carrying out my work.

Last but not the least I am thankful to the All Mighty for giving me enough perserverance, patience and strength to rise after every debacle.

Ajit Kumar Sahu

Dedicated to My Parents and Teachers

Abstract

The design and manufacture of dies/tools for producing sheet metal components is extremely costly and time consuming. The high cost and long lead-times of die design/development and manufacture are mainly due to the traditional trial and error procedures used by skilled die designers and makers to obtain the correct tooling shape and forming conditions that will yield the desired part shape and properties. The design phase of dies/tools for a given component involves several calculations and subsequent decisions based on heuristics and existing trade practices in industry. A process planner may have to spend lot of time in analyzing the given problem and/or in consulting the handbooks for various relations to arrive at desired solution. Furthermore, the designed die quality will be dependent on process planner's skill and experience. To overcome above mentioned problems and to sustain competitiveness, there is a need for an intelligent aid to the process planner.

Review of the published literature reveals that there have been few attempts to develop an aid to the process planner to decide about the process sequence. However, those attempts are mainly based on expert system related to the limiting drawing ratio, sequencing etc. besides complicated way of object modeling. Development of an expert system regarding the formability limits of commonly deep drawn materials, for the range of process parameters used in the deep drawing process is very difficult. Therefore, an attempt is made in the present work to develop a knowledge based process planning system which uses the geometric primitives to model the object in conjunction with an analytical model to estimate limiting drawing ratio for first as well as subsequent draws to produce the required geometry.

An attempt is made to develop a Knowledge-based process planning system for axisymmetric deep drawing. Parametric object modeling using geometric primitives for feature based geometric description makes the input of geometric information to the system easier. Required database was developed for material properties, tribological data and presses. Die design rules have been implemented to give the die arc and punch radii at each stage of drawing. The objective of the system is to generate all feasible operation sequences. through which the desired cup specified can be produced. The number of stages is determined by the process analysis model developed by Sonis[2001], which estimates the limiting drawing ratio for first as well as subsequent draws. The knowledge based system developed generates all feasible process sequences considering formability limits and the rules in the database. User can select the best among them.

Contents

List of Figures	iii
List of Tables	v
Nomenclature	vii
1 Introduction and Literature Survey	1
1.1 Introduction	1
1.2 Deep Drawing Process	2
1.2.1 Redrawing	4
1.3 Drawability	5
1.4 Knowledge Acquisition from Experts	6
1.5 Process Planning	6
1.5.1 Definition	6
1.5.2 Process Planning Approaches	6
1.6 Literature Survey	7
1.7 Scope and Objective of the Present Work	11
1.8 Organization of the Thesis	12
2 Knowledge-Based System	15
2.1 Introduction	15
2.2 Object Modeling and Interfacing	16
2.2.1 Blank Size Calculation	18
2.3 Elementary Design Rules	20
2.4 Databases	21
2.4.1 Material Properties	22
2.4.2 Tribological Data	22
2.4.3 Presses	23
2.5 Process Analysis	24
2.5.1 Draw Analysis	26

3	System Implementation	33
3.1	Introduction	33
3.2	Object Modeling	33
3.3	Databases	34
3.3.1	Selection of Material	35
3.3.2	Selection of Lubricant	35
3.3.3	Selection of Press	36
3.4	Process Sequence Design Module	36
3.5	Viewing the Results	37
4	Results and Discussion	39
4.1	Introduction	39
4.2	Validation	39
4.3	Case Studies	44
4.3.1	Input Parameters to the System	45
4.3.2	Output from the System	45
4.3.3	Case I	46
4.3.4	Case II	46
4.3.5	Case III	48
4.3.6	Case IV	49
4.4	Journey Through the System	53
5	Conclusions and Scope for the Future Work	57
5.1	Conclusions	57
5.2	Scope for the Future Work	58
	References	59
	Appendix A	63

List of Figures

1.1	Drawing of a cup-shaped part: Symbols c = clearance, D_0 = blank diameter, D_p = punch diameter, r_d = die arc radius, r_p = punch corner radius, F = drawing force, F_h = blank-holding force.	3
1.2	Stages in deformation of work in deep drawing: (1) punch makes initial contact with work, (2) bending, (3) straightening, (4) friction and compression, and (5) final cup shape showing effects of thinning in the cup walls. (v = velocity of punch, F = punch force, F_h = blank-holding force)	3
1.3	Redrawing of a cup: (1) start of redraw and (2) end of stroke. (v = velocity of punch, F = punch force, F_h = blank-holding force)	5
1.4	Modes of Fracture in Cup Drawing [El-Sebaie and Mellor, 1972]	13
1.5	Thickness profiles of drawn cups [El-Sebaie and Mellor, 1972]	14
2.1	Block Diagram of knowledge Based Process Planning System	16
2.2	Element library	17
2.3	Cross section of an axisymmetric cup	19
2.4	Table of possible elements	20
2.5	Schematic representation of cup drawing, showing the co-ordinate system and dimensional notations.	26
2.6	Force acting on the Die Arc Region	27
2.7	Radial stresses in the flange element	28
2.8	Section of a partial drawn cup	30
2.9	Redrawing of Cups	30
3.1	Main window	34
3.2	Object modeling	35
3.3	Material database	36
3.4	Process Sequence Design Flow Chart	38
4.1	Variation of LDR with normal anisotropic value for flat bottom cups drawn from soft Aluminum. ($\bar{\sigma}_e = 118(\bar{\epsilon}_e)^{0.227}$ MPa, $\sigma_y = 28.8$ MPa, $r_{cf} = 50.8$ mm, $r_d = 8.635$ mm, $t_0 = 1.016$ mm)	40

4.2	Variation of LDR with normal anisotropic value for flat bottom cups drawn from AA 3003. ($\bar{\sigma}_e = 157.1(\bar{\epsilon}_e)^{0.235}$ MPa, $\sigma_y = 41$ MPa, $r_{cf} = 50.8$ mm, $r_d = 8.635$ mm, $t_0 = 1.016$ mm)	41
4.3	Object modelling using geometric primitives	53
4.4	Material selection	54
4.5	Lubricant selection	54
4.6	Operating parameters	55
4.7	Realtime decision for annealing	55
4.8	Process plan without annealing	56
4.9	Process plan with annealing	56

List of Tables

2.1	Punch to die clearance for drawing operations, ASM Handbook [1992]	22
2.2	Alloy types: AA 3003 aluminum alloy, others are steel alloys, DDQ-deep drawing quality; CA-continuous annealing; BA-batch annealing	22
2.3	Hyphenation indicates that several components are used in the lubricant. EM - emulsion (the listed lubricants are emulsified and 1-20% dispersed in water); EP - extreme pressure compounds (containing S,Cl and / or P); FA - fatty acids, alcohols amines and esters; MO - mineral oil; PC - polymer coating	23
2.4	Alloy types: AA 3003 aluminum alloy, others are steel alloys, DDQ-deep drawing quality; CA-continuous annealing; BA-batch annealing	23
4.1	Comparison of experimental data and predictions of the model presented by Sonis [2001] for mild steel sheets. ($\bar{\sigma}_e = 617(\bar{\epsilon}_e)^{0.310}$ MPa, $\sigma_y = 200$ MPa, $r_{cf} = 50$ mm, $r_d = 8.5t_0$, $t_0 = 1$ mm) Experiment were carried out by Whiteley [1960].	41
4.2	Comparison of experimental and theoretical data of LDR for non ferrous sheets. lubricant : Droyt-Sol 4M, mineral oil. $\mu = 0.10$, $r_{cf} = 19.6225$ mm, $r_d = 7.450$ mm. Experiment was carried out by El-Sebaie and Mellor [1972].	42
4.3	Comparison of theoretical data of LDR for Redraws without intermediate annealing with Lange [1985] suggested drawing ratio. Sheet metal thickness, $t_0 = 1.0$ mm. <i>Source: Handbook of Blanking Technology, Romanowski [1959]</i>	43
4.4	Comparison between the predictions of the model presented by Sonis ¹ [2001] and limiting drawing ratios suggested by www.ici.net/cust-pages/harddro.html ² , [1996]. SAE 1006 ($\bar{\sigma}_e = 617(\bar{\epsilon}_e)^{0.310}$ MPa, $\sigma_y = 200$ MPa), DQ Killed ($\bar{\sigma}_e = 610(\bar{\epsilon}_e)^{0.22}$ MPa, $\sigma_y = 172$ MPa), DQ Rimmed ($\bar{\sigma}_e = 619(\bar{\epsilon}_e)^{0.21}$ MPa, $\sigma_y = 207$ MPa), $r_{cf} = 50$ mm, $r_d = 8.5 * t_0$, $t_0 = 1$ mm	44
4.5	Process plan output (Case I)	47
4.6	Process plan output (Case II)	47
4.7	Process plan output without annealing (Case III)	48
4.8	Process plan output with annealing after first draw (Case III)	49
4.9	Process plan output without Annealing ($t_0 = 1.0$ mm)	50
4.10	Annealing after first draw	50
4.11	Annealing after second draw	51

4.12 Annealing after third draw	51
4.13 Process plan output (Case IV)	51
4.14 Process plan output without Annealing($t_0 = 1.5$ mm)	52
4.15 Annealing after first draw ($t_0 = 1.5$ mm)	52
4.16 Annealing after second draw ($t_0 = 1.5$ mm)	53

Nomenclature

C_1, C_2, C_3, C_4, C_5	constants
D_0	initial blank diameter
D_p	punch diameter
DR	drawing ratio
F_w	flange width
F	drawing force
F_h	blank-holding force
H	final height of the cup
K	material constant
$L_i : i = 1, 2, 3..$	length around the axis of rotation for the cup elements
LDR_0	limiting drawing ratio for the first draw
$LDR_i : i = 1, 2, 3..$	limiting drawing ratio for redraw
P_c	critical drawing force during first draw
P_{c_2}	critical drawing force during redraw
$P_i : i = 1, 2, 3..$	path of center of gravity for the cup elements
P_r	radial drawing force in the flange region
$P_{r_{cd}}$	radial drawing force at the radius r_{cd}
R	initial radius of the annular ring
\bar{R}	normal anisotropy value
R_0	initial blank radius
R_1, R_2	intermediate radius on initial blank
$R_i, R_{i+1} : i = 1, 2, 3..$	intermediate radius on the bottom of the cup
SA	surface area
t	instantaneous thickness
t_0	initial blank thickness
r	radius of the partially drawn cup corresponding to R
r_d	die arc radius
r_0	radius of the partially drawn cup corresponding to R_0
r_{c_0}	cup radius after the first draw
$r_{c_i} : i = 1, 2, 3..$	cup radius after redraws
r_{cd}	die opening radius
r_{cf}	final cup radius
r_{pf}	final punch corner radius
r_{df}	final die arc radius

v	velocity of punch
n	strain hardening exponent
μ	coefficient of friction
$\bar{\epsilon}$	generalised strain
$\epsilon_r, \epsilon_\theta, \epsilon_z$	strains in the x, y & z directions respectively
$\bar{\epsilon}^0$	strain induced during first draw
$\bar{\epsilon}^i : i = 1, 2, 3..$	strain induced during redraws
$d\epsilon_r, d\epsilon_\theta, d\epsilon_z$	strain increments in the x, y & z directions respectively
$\bar{\sigma}_e$	generalised stress
σ_y	yield stress
$\sigma_r, \sigma_\theta, \sigma_z$	stresses in the x, y & z directions respectively
$\sigma_{r_{cd}}$	radial stress at the radius r_{cd}
σ_{r_0}	radial friction stress during first draw
$\sigma_{r_{i-1}}^{II}$	radial friction stress during redraw
$\sigma_{r_i} : i = 1, 2, 3..$	radial friction stress during redraws
σ_r^{II}	radial drawing stress during redraw

Chapter 1

Introduction and Literature Survey

1.1 Introduction

In today's competitive world there is an increasing need of high quality components produced at lower cost. Deep drawing is a process in which a blank or workpiece, usually controlled by pressure plate, is forced into and/or through a die by means of a punch to form a hollow component in which the thickness is substantially the same as that of the original material. For producing most of the deep drawing components multiple draws are required. The design and manufacture of dies/tools for producing deep drawing components is extremely costly and time consuming. It is necessary to cut down the time for developing, designing and producing the dies/tools for the production of sheet metal components so as to stay competitive in the global economy. The high cost and long lead-times of die design and manufacture are mainly due to the traditional trial and error procedures used by skilled die designers and makers to obtain the correct tooling shape and forming conditions that will yield the desired part shape and properties. The design phase for a given component involves several calculations and subsequent decisions are based on heuristics and existing trade practices in industry. A process planner may have to spend a lot of time in analyzing the given problem and/or in consulting the handbooks for various relations to arrive at the desired solution. Furthermore, the designed die quality will be dependent on process planner's skill and experience.

To overcome the above mentioned problems and to sustain competitiveness, there is a need for an intelligent aid to the process planners. Generation of a process plan needs a model, which should be based on the science of the deep drawing process. Modeling in its initial form can be seen as an aid in understanding the process and its parameters. Without the complete knowledge of the influence of the variables such as material property variations, friction conditions, punch/die geometry and work piece geometry on the process mechanics, it will not be possible to predict and prevent the defects or to design the equipment adequately. For generating an automatic process sequence design, there is a need for the development of computer model that uses the design knowledge and properties available from the hand-

books. This computer model should incorporate a process analysis module (based on the force equilibrium method) so that it can help to retain the 'know-how' in the company even if the designer leaves. It will also help in standardization of design practices. Stage design and process planning for the manufacture of sheet metal components by single and multi-stage deep drawing requires knowledge of limiting drawing reduction (LDR).

Number of approximate methods of analysis have been developed and applied to various metal forming processes. The most well known methods are the slab method, slip line field method, upper bound method and finite element method. Upper bound and slip-line field methods require the assumption of kinematically admissible velocity and statically admissible stress fields respectively. In finite element method, the domain of interest is divided into a number of suitable elements and the governing differential equations of the system are reduced to algebraic equations by using appropriate approximations for the field variables over the elements. Finite element analysis can predict more accurate forming loads and determines the effect of various process parameters on the metal flow. The models based on the finite element method are intensively time consuming. Therefore in the present work a model based on the force equilibrium method has been used to estimate the limiting drawing ratio.

Present work aims at developing a knowledge-based process planning system for axis-symmetric deep drawing. It incorporates the object modeling (feature based geometric description) to obtain the required blank size, process analysis model to estimate the limiting drawing ratio for single and multi-stage deep drawing considering various aspects such as anisotropy, plastic instability, material property variation, etc. of the given material. Development of a knowledge-based process planning system will help process planners in developing and evaluating process sequences and in predicting possible defects/problems before the actual dies/tools are manufactured. Ability to predict and prevent problems will allow prior modification of the process sequence/tool design with obvious financial and time saving. Additional advantages are that more accurate and consistent plans can be generated.

1.2 Deep Drawing Process

Drawing is a sheet-metal forming operation used to make cup-shaped, box-shaped, or other more complex-curved, hollow-shaped parts. It is performed by placing a sheet-metal blank over a die cavity and then pushing the metal into the opening with a punch, as shown in Figure 1.1. The blank must usually be held down flat against the die by a blank holder.

A blank of diameter D_0 is drawn into a die by means of a punch of diameter D_p . The punch and die have corner radii, r_p and r_d . The sides of punch and die are separated by a clearance which is about 10% greater than the stock thickness. The punch applies a downward force F to accomplish the deformation of metal, and a downward holding force F_h is applied by the blank holder to prevent wrinkling, as shown in the Figure 1.1.

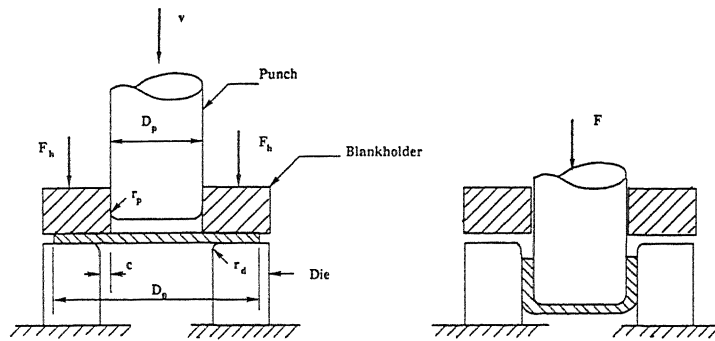


Figure 1.1: Drawing of a cup-shaped part: Symbols c = clearance, D_0 = blank diameter, D_p = punch diameter, r_d = die arc radius, r_p = punch corner radius, F = drawing force, F_h = blank-holding force.

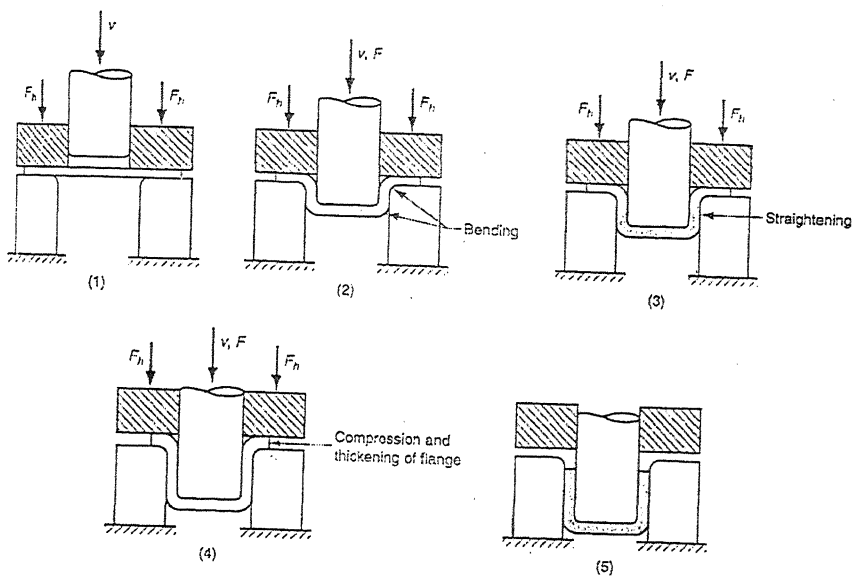


Figure 1.2: Stages in deformation of work in deep drawing: (1) punch makes initial contact with work, (2) bending, (3) straightening, (4) friction and compression, and (5) final cup shape showing effects of thinning in the cup walls. (v = velocity of punch, F = punch force, F_h = blank-holding force)

As the punch proceeds downward towards its final bottom position, the work experiences a complex sequence of stresses and strains as it is gradually formed into the shape defined by the punch and die cavity. The stages in the deformation process are illustrated in Figure 1.2. As the punch first begins to push into the work, the metal is subjected to bending operation. The sheet simply bent over the corner of punch and the corner of the die, as in the Figure 1.2(2). The outside perimeter of blank moves in toward the center in this stage, but only slightly.

As the punch moves further down, a straightening action occurs in the metal that was

previously bent over the die radius, as shown in Figure 1.2(3). The metal at the bottom of the cup as well as along the punch radius, moves downward with the punch. But the metal that was bent over the die radius is straightened to form the wall of the cylinder. At the same time, more metal must be added to replace that which is now being used in the cylindrical wall. The metal in the flange portion of the blank is pulled or drawn toward the die opening to resupply the previously bent and straightened metal now forming the cylinder wall. During this stage of the process, the friction and compression play roles in the flange of the blank. Initially static friction is involved until the metal starts to move and then, sliding friction governs the process. Magnitude of the holding force applied by the blank holder as well as the friction conditions at the two interfaces are determining factors in the drawing operation. Lubricants are generally used to reduce friction forces. In addition to friction, compressive forces also occur on the outer edge of the blank. As the metal in this portion of the blank is drawn toward the center, the outer perimeter becomes smaller. As the volume of metal remains constant, the metal is squeezed and becomes thicker at the flange edge. This often results in wrinkling of the remaining flange of the blank, especially when thin sheet metal is drawn or when the blank holder force is too low. It is a condition that cannot be corrected once it has occurred. The friction and compression effects are illustrated in Figure 1.2(4).

The holding force applied by the blank holder also plays an important role in deep drawing. If it is too large, it prevents the metal from flowing properly toward the die cavity, resulting in stretching and possible tearing of the sheet metal. Determining the proper holding force involves a delicate balance between these opposing factors. Progressive downward motion of the punch results in a continuation of metal flow caused by drawing of cylinder wall, as shown in the Figure 1.2(5).

1.2.1 Redrawing

Redrawing facilitates the production of deeper and narrower cups and/or stepped cups. The first drawing operation cannot produce a cup because of limiting drawing ratio thus redrawing has to be employed. Utilizing redrawing, the compressive stresses are reduced due to the fact that the radial stress, which generates them are small. Hence, the load that the wall has to transmit is been lowered. Stepped or complex draws are obtained in a fashion similar to flanged cups in cupping. A redrawing operation is illustrated in Figure 1.3.

Conditions exists during redrawing are:

- As the metal flows it must be compressed, but only between the old punch radius and the new die radius. This is where wrinkling may occur, so a tubular blank holder is used between the punch and inner diameter of drawn cup.
- The cylindrical wall and the top edge of the drawn cup simply slip downward on the blank holder. No work-hardening occurs at this time.

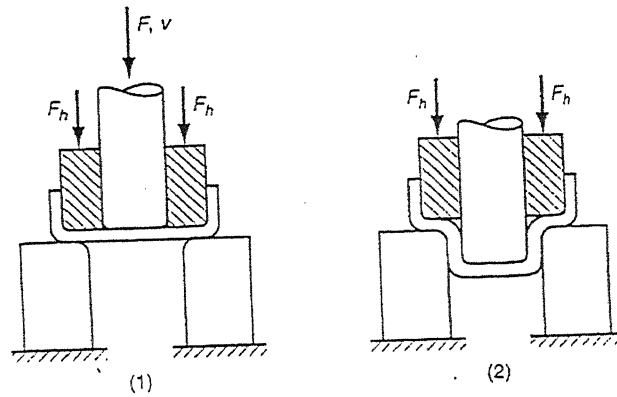


Figure 1.3: Redrawing of a cup: (1) start of redraw and (2) end of stroke. (v = velocity of punch, F = punch force, F_h = blank-holding force)

- The most outstanding change is that the cylindrical wall must be bent over the blank holder radius and then straightened. This is in addition to the later bending to the die radius and straightening.

The percentage of reduction in diameters for all redraw operations are considerably less than that of the first draw due to the following reasons:

- The new cup side wall area taking the tensile loading is much smaller and will tear at lower punch loads. This new load-bearing metal was formed from the soft metal bottom of the drawn cup and has no strength advantage from previous work hardening.
- The metal in the drawn-cup cylindrical wall is already work hardened and has lower ductility for the redraw. Annealing before redraw will restore full ductility at added cost.

1.3 Drawability

Drawability of any material is expressed in terms of a Limiting Drawing Ratio (LDR) or Percentage Reduction. LDR is defined as the ratio of diameter of the largest blank that can be successfully drawn without fracture D_0 to the diameter of the punch D_p . Therefore,

$$LDR = \frac{D_0}{D_p}$$

and the Percentage Reduction is given by

$$\% \text{ Reduction} = \frac{D_0 - D_p}{D_0} \times 100$$

In an idealized forming operation deformation occurs in the flange and over the die lip. No deformation takes place over the nose of punch. The drawability of metal depends on two factors:

1. The ability of the material in the flange region to flow easily in the plane of the sheet under shear.
2. The ability of the side wall material to resist deformation in the thickness direction.

1.4 Knowledge Acquisition from Experts

The power of a 'knowledge-based' system as the name implies, often lies in the strength of its knowledge. The acquisition of knowledge and the representation of knowledge are two of the most important tasks in the construction of expert systems. Knowledge acquisition is essentially collecting knowledge, experience, rules-of-thumb or empirical rules, and other important relevant information from experts or other reliable sources. In the present work, information found in the open literature was reviewed and the available knowledge is used to form the knowledge base.

1.5 Process Planning

1.5.1 Definition

Process planning is the function within the manufacturing facility that establishes which manufacturing processes and parameters are to be used (including machines which are capable of performing these processes) to convert a piece of part from its initial form to its final form. This is usually predetermined by the design engineer and indicated on engineering drawings. Process planning links design with manufacturing of a product and the process plan contains factors like functional requirements of the product, the output volume, the operations, tools and equipment necessary, and the estimated manufacturing cost for producing the product. In spite of the importance of process planning in manufacturing cycle it is still predominantly a manual activity, leaning heavily on experience, skill and intuition. Dependence on practical experience often precludes a thorough analysis and optimization of the process plan and nearly always results in higher-than-necessary production costs, delays, errors and non-standardization of processes. The desire to increase quality and reduce lead time and cost, or to improve productivity has lead to Computer-Aided Process Planning (CAPP).

1.5.2 Process Planning Approaches

The approaches used for computer aided process planning (CAPP) can be classified as: the *variant approach*, and the *generative approach*. However, with the rapid development of new

techniques, many CAPP systems do not easily fit this classification since they combine both approaches.

Variant Approach

In the variant approach, a process plan for a new component is created by retrieving a standard plan that has been stored in the database, using group technology concepts like classification and coding with some modification. In some variant systems, parts are grouped in a number of part families, characterized by similarities in manufacturing methods, thus related to group technology. For each part family a standard process plan, which includes all possible operations for the family is stored in the system. The standard plan is retrieved and edited for the new part.

Generative Approach

Generative process planning can be concisely defined as a system that synthesizes process information in order to create a process plan for a new component automatically. In this system, process plans are created from information available in a manufacturing database without human intervention. On receiving the design model the system can generate the required operations and their sequence for the component. Ideally, a generative process-planning system is a turnkey system with all the decision logic coded in the software. The biggest advantage of this approach is that it is fully automatic and does not rely on specific expertise of the process planner.

1.6 Literature Survey

Deep drawing, with *press working*, *stamping* and *die forming* being commonly used synonyms, is an experienced-based technology. A natural procession of investigation starts with an experimental study from which analytical models can be developed. 'Know-how' has been accumulated largely by trial and error, since the process was introduced in 18th century, though a massive thrust to understand the process started only in 1920's.

Chung and Swift [1951] measured changes in the thickness undergone by a uniformly thin blank when drawn into a cup and tried to predict the drawing force. They carried out a comprehensive experimental and analytical investigation at the University of Sheffield in 1950. They drew 4 inch diameter cups of varying blank sizes, thickness, wall recess radii, materials and operating conditions with each undergoing a total of 500 to 900 measurements. The analytical treatment utilized some of Hill's [1950] predictions as applied to the strains developing in radial drawing. They also developed a model for bending over the die profile radius. They were, however unable to extend their solution to the punch nose region. Wallace [1960] carried out experiments with finished punch and knurled punch with and without lubrication in

order to observe the increment in limiting drawing ratio. He obtained an increase in limiting drawing ratio from 2.325 with a polished and lubricated punch to 2.550. These experiments were carried out on E.D.D. (Extra Deep Drawing) quality and D.D. (Deep Drawing) quality steels.

Wright [1962] studied the effect of mechanical properties (ultimate tensile strength, % elongation, strain hardening and normal anisotropy) on deep drawability and stretch formability for various materials viz. commercial aluminum, copper, zinc and titanium and its alloys. He concluded that relationship between deep drawability and the four mechanical properties cannot be expressed in terms of a product/quotient type of empirical formula.

Woo [1968] presented the analysis of the deep drawing of a cylindrical cup including the drawing and stretch-forming parts. In the analysis, he calculated the strains due to drawing near the die lip and used them as the boundary values for the analysis of the stretch-forming region. He also analyzed the effect of anisotropy using the Hill's theory for anisotropic material [Hill, 1950].

El-Sebaie and Mellor [1972] showed the effect of anisotropy value (\bar{R}) and strain-hardening exponent n -value on limiting drawing ratio. Their results indicate two instability modes, one in the cup wall and the other in the flange. Experiments were conducted on three materials viz. soft aluminum, half hard aluminum and soft 70/30 brass drawn with smooth punch as well as rough punch to determine the limiting drawing ratio. Figures 1.4 and 1.5 shows the modes of fracture and the thickness distribution of the drawn cups respectively. The small arrows in the Figure 1.5 point to the junction of the punch profile and punch stem, and the large arrows indicate the fracture position when drawing oversize blanks. They also developed a theoretical model based on the slab method and used the finite difference method to determine the stress and strain distributions in the cup. The predicted value of limiting drawing ratio was not close to the experimental values.

Korhonen [1982] developed a model based on the slab method for estimating the maximum drawing force during deep drawing of cylindrical cups with flat-nosed punch. He used the load maximum principle for localization of plastic flow to estimate the drawing force for two cases, one for plane stress state when thickness/punch profile radius was small, and the other for tri-axial stress using the free body diagram (slab method). He obtained the value for press load (drawing force, P_d) as,

$$P_d = P_c \frac{DR - 1}{LDR - 1}$$

where DR is drawing ratio and P_c is the critical drawing load at LDR .

Several attempts [Yu and Johnson, 1982 and Meier and Reissner, 1983] have been made to solve the buckling problem of annular ring. Yu and Johnson [1982], proposed the critical conditions for elastic and plastic buckling of flange having circular shape, based on a two-dimensional buckling model. Meier and Reissner [1983] investigated the effect of stress

distribution, thickness distribution and normal anisotropy on the stability behavior of circular flange. They used Rayleigh quotient (ratio of bending energy to membrane energy) for determining the formation of folds. If the ratio is greater than one, the flange remains flat whereas for values less than one, folding of flange takes place. Oskada et al. [1995] proposed a model based on the finite element method for determining the optimal history of the blank holding force which will not cause wrinkling and localized thinning for each deformation step. They determined the blank holding force in deep drawing of an aluminum sheet. The minimum holding force required to prevent the occurrence of wrinkles was investigated by Kikuchi [1949], taking the anisotropic effect into consideration. Miyagawa [1957] reported a series of articles on the mechanism of wrinkling in deep drawing using energy method, and Kawai [1961] discussed the critical condition of wrinkling by use of the moment equilibrium for the cases with and without a blank holding plate [Source: Fukui and Kobayashi [1966]]. Ahmetoglu et al. [1995] determined the wrinkling and fracture limits. They performed experiments to show the effect of blank-holding force on the fracture and wrinkling of rectangular pans. The rectangular pans were formed from aluminum alloy 2008-T4. Siegert et al. [1995] developed a closed loop control system to control flow of material between the lower and upper binder plate of the single action press in such a manner that prevents the occurrence of both tears and wrinkles in drawn part. Sensors were mounted to measure the blank holder force and the flow-in of material in the die to maintain the blank holder force in the working region. Much of the emphasis was paid on the correlation of LDR of a sheet metal with its material properties especially with the normal anisotropy value, which indicates better drawability when its value is large. Many investigations have been carried out to evaluate the limiting drawing ratio, mainly for the first stage. Wilson et al. [1966] investigated the effect of size of blank on the load required to fracture the base of cup. The experiments were conducted on low carbon steel, α -titanium, zinc, and 3/4 hard aluminum to predict the anisotropy value from LDR values. Atkinson [1967] applied the technique of curve fitting to get the empirical relation from the experimental data for limiting drawing ratios of various materials ranging from mild steel to titanium. The general relationship between LDR and \bar{R} was given by

$$8 \text{Log}\left(\frac{D_o}{d}\right) = \text{Log} \bar{R} + 3$$

Emani [1984] reported that the plastic flow of anisotropic sheet during deep drawing may be regarded a two-stage deformation process, both stages occurring simultaneously. First stage deformation, taking place in the cup wall, being controlled by normal anisotropy. While the second stage deformation or asymmetric flow due to planar anisotropy, being responsible for the change in shape of rim of the flange of a partially drawn cup from circular to hypotrochoid.

Reissner and Ehrismann [1987] used the simulation technique based on the finite difference method to show extreme dependence of LDR on coefficient of friction (μ). Material was assumed to be rigid plastic with normal anisotropy and work hardening characteristics.

Leu [1997] developed an expression, based on Hill's theory of anisotropic plasticity. He showed the effects of normal anisotropy (\bar{R}) and strain hardening exponent (n) on limiting drawing ratio and estimated the maximum drawing load at a certain drawing ratio, limiting drawing ratio (LDR) was obtained as

$$LDR = \sqrt{e^{(2fe^{-n}\sqrt{\frac{1+\bar{R}}{2}})} + e^{(2n\sqrt{\frac{1+\bar{R}}{2}})} - 1}$$

where f is the factor of drawing efficiency varying with sheet thickness, tooling, lubrication, etc. Equation used for evaluating the drawing load was

$$\frac{P_d}{P_c} = \frac{\ln(DR^2 + 1) - 0.7}{\ln(LDR^2 + 1) - 0.7}$$

Leu [1999] continued his work and developed an expression for determining LDR. It normally estimates the critical blank size for a given cup radius. He has given an expression, which is a function of process parameters like normal anisotropy, strain hardening exponent, coefficient of friction, yield strength of material, etc. He showed the effect of these parameters on LDR and compared his results with the experiments for the first stage only.

Literature review for the first draw reveals that many of the researchers primarily concentrated to show the effects of material characteristics, such as the normal anisotropy value \bar{R} , strain-hardening exponent n , the friction coefficient $[\mu]$ on the LDR. Recently, Sonis [2001] presented a process analysis model to determine the LDR for the first draw as well as for redraws.

Fogg [1968] studied bending and straightening of the unconstrained region in redrawing through a conical die by applying linearization of von-Mises yield criteria for plane stress. He showed through his experiments, bending and unbending stresses account for 23% and 47% of the total stress for redrawing ratios of 1.14 and 1.6, respectively.

Parsa et al. [1994] used a rigid-plastic finite element simulation based on the theory of plasticity for slightly compressible materials to compare the limiting drawing ratio achievable by forward and reverse redrawing processes. In their analysis they used four layers of isoparimetric rectangular elements and concluded that direct redrawing allows for higher total drawing ratios than reverse redrawing. Furthermore, they showed that the limiting drawing ratio for the second stage decreases and the total achievable drawing ratio increases with increasing first stage drawing ratio.

Min et al. [1995] analyzed axisymmetric multi-stage deep drawing operation using rigid-plastic finite element method and bilinear quadrilateral elements. They obtained loads on punches/dies and predicted variations in thickness strains at each stage.

Sonis [2001] presented a process analysis model to determine the LDR for the first draw as well as for redraws considering the effects of normal anisotropy, co-efficient of friction, strain hardening, die arc radius, thickness of sheet and substantiated with available experimental results in literature.

For designing automated process sequence, many researchers [Eshel et al., 1986; Sitaram et al., 1991; Doege and Schulte, 1992; Tisza, 1995 and Esche et al., 1996] have developed the Computer-Aided Engineering (CAE) systems using the Knowledge-based rules and known formulations for the calculations of drawing load.

Eshel et al. [1986] developed rule based modeling for axisymmetrical deep drawing. They used the contemporary knowledge for single stage as well as for redrawing in rule form that can be directly utilized in an automated process-planning procedure. It incorporates empirical formulations, press working practice and plasticity knowledge.

Sitaram et al. [1991] developed a hybrid Computer- Aided Engineering system. The input to the system is the final sheet metal object geometry that needs to be manufactured and output from the system is the process sequence with intermediate object geometries. However, the database constructed to check the maximum diameter reduction of the sheet blank was based on the hypothesis that materials whether they are high ductile, medium ductile or low ductile exhibit almost similar forming-limit characteristics.

Tisza [1995] developed a Knowledge Based Expert System for metal forming to generate process plans. Esche et al. [1996] developed an analytical module based on the Finite Element Method (FEM) called SECTIONFORM to predict potential problems by simulating the forming processes. Esche et al. [2000] extended their work to handle forward and reverse drawing operations. They compared their punch travel and true strains results with the three-dimensional sheet forming analysis program PAM-STAMP for aluminum cups.

Toh et al. [1995] developed a PC-based flat patterning system that runs on AutoCAD to determine the blank shapes and sizes

Rao [1998] developed a parameter optimization module for CAPP of deep drawing using a combination of variant generative approaches. The objective function was to minimize the overall power in multi-stage drawing. The diametrical reduction was decided by the critical punch load. His results indicate that the overall power does not vary significantly with number of stages.

1.7 Scope and Objective of the Present Work

Critical review of the published literature reveals that there have been few attempts to develop an aid to the process planner to decide about the process sequence. However, attempts made by Sitaraman et al. [1991] and Tisza [1995] are mainly based on expert system related to the limiting drawing ratio, sequencing etc. besides complicated way of object modeling. Development of an expert system regarding the formability limits of commonly deep drawn materials, for the range of process parameters used in the deep drawing process is very difficult. Formability limits of deep drawn materials requires the complete knowledge of the influence of the variables such as material property variations, friction conditions, punch/die and work-

piece geometry on the process mechanics. Literature survey also reveals that attempts have been made to establish the relationship between normal anisotropy, strain hardening exponent, die arc radius and deep drawability for the first stage. Recently, Sonis [2001] presented a process analysis model to determine the LDR for the first draw as well as for redraws considering the effects of normal anisotropy, co-efficient of friction, strain hardening, die arc radius and thickness of the sheet. Therefore, the objective of the present work is to develop a knowledge based process planning system which uses the geometric primitives to model the object in conjunction with an analytical model to estimate limiting drawing ratio for first as well as subsequent draws to produce the required geometry. The other objectives are

- Parametric modeling of the input geometry.
- Development of databases for material properties, friction coefficient, press data etc.
- Generation of all feasible process sequence considering formability limits and rules in the database.

1.8 Organization of the Thesis

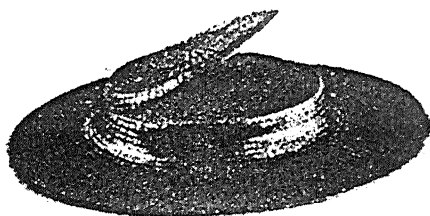
Brief discussion on the deep drawing process has been presented in chapter 1. Scope and objective of the present work is presented in this chapter. The organization of the thesis report is as follows:

Chapter 2 presents the different aspects of the knowledge based system and analytical model developed by Sonis[2001].

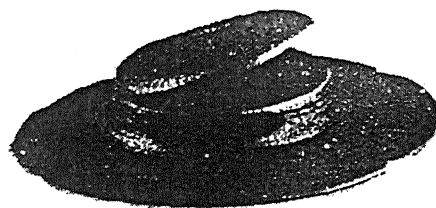
Chapter 3 deals with the implementation of the knowledge based system.

Chapter 4 compares the predictions of the model developed by Sonis[2001] with the available experimental results for first draw as well as for redraws. Also, presents the case studies to demonstrate the capabilities of the presented system.

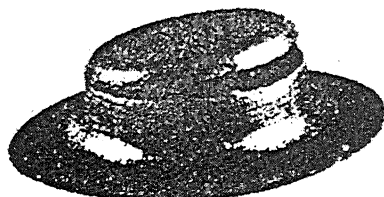
Chapter 5 concludes the present work with scope for the future.



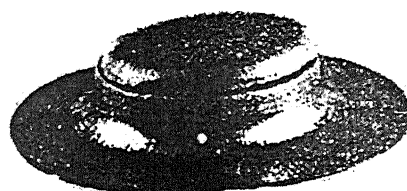
HH.Al, Smooth Punch
 DR = 2:063
 LDR = 2:053



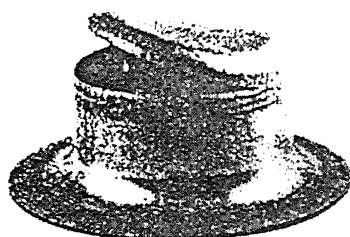
HH.Al, Rough Punch
 DR = 2:105
 LDR = 2:100



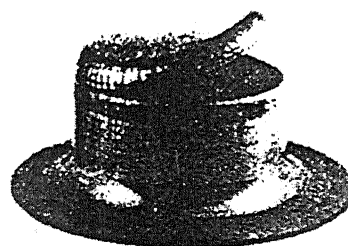
Soft Al, Smooth Punch
 DR = 1:974
 LDR = 1:963



Soft Al, Rough Punch
 DR = 2:063
 LDR = 2:053



Soft 70/30 Brass, Smooth Punch
 DR = 2:126
 LDR = 2:116



Soft 70/30 Brass, Rough Punch
 DR = 2:200
 LDR = 2:19

Figure 1.4: Modes of Fracture in Cup Drawing [El-Sebaie and Mellor, 1972]

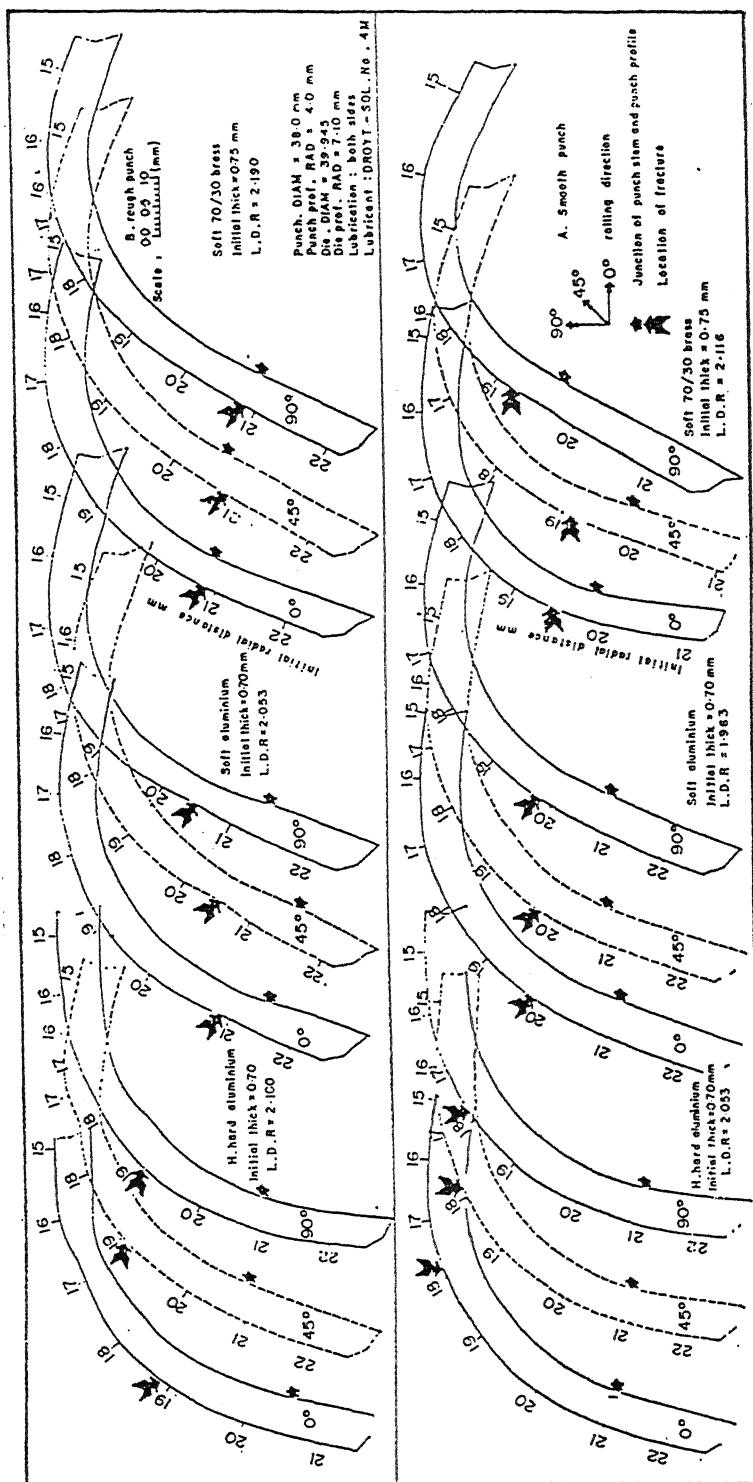


Figure 1.5: Thickness profiles of drawn cups [El-Sebaie and Mellor, 1972]

Chapter 2

Knowledge-Based System

2.1 Introduction

With the widely accepted use of computer-aided design/manufacturing (CAD/CAM) die manufacturing has been extensively computerized. The present trends now are to improve die and process design methods by modeling and optimizing various deformation processes. Also to establish an integrated design and manufacturing activity that utilizes not only modeling techniques but also knowledge based systems for preliminary die design and selection of initial process conditions. Knowledge based systems may be defined as a computer based system that uses an explicit representation of knowledge, facts and reasoning techniques to solve problems that normally require the abilities and skill of human expertise. A typical knowledge based system consist of

- A knowledge acquisition facility that receives and collects rules and facts from human experts in a specific area of expertise. Such facility may also include a "rule editor", allowing the improvement of existing and addition of new rules by the user.
- Data bases to store facts and rules usually with interfaces to other data base systems.
- An inference engine that determines how to apply the knowledge rules to solve a problem.
- A user interface that allows the user to utilize the knowledge based system for solving specific problems.

The general architecture of a knowledge-based process planning system for axi-symmetric deep-drawn components has been developed, as shown in the Figure 2.1. The main parts of this system are as follows:

- Object modeling and interfacing: For the parametric modeling of the input geometry.

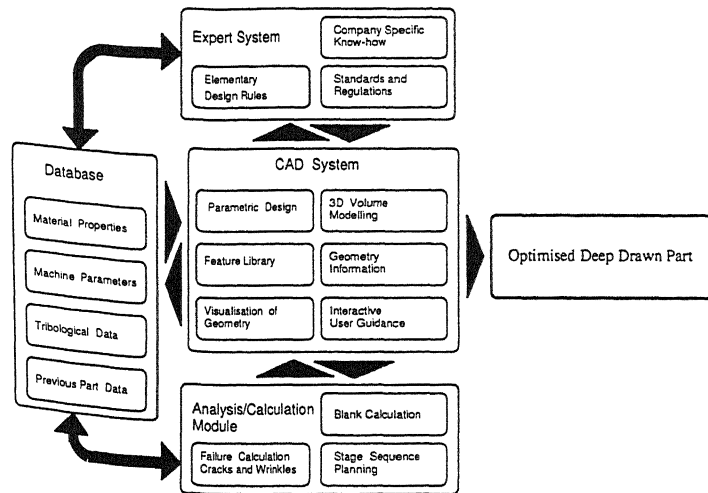


Figure 2.1: Block Diagram of knowledge Based Process Planning System

- Database : Database of the knowledge based system basically contains the material properties, tribological data, press data as well as design rules.
- Analysis Module : The analysis model developed by Sonis[2001] is used for the prediction of LDR.
- Expert system : This module consists of the elementary design rules for designing the die and punch radius etc.

2 Object Modeling and Interfacing

The final object geometry for which a process sequence needs to be designed is the input to the system. The following sections describe briefly the various methods available for inputting the geometric information to the knowledge-based system.

- Primitive-based input : In this technique complicated cross-sections can be decomposed into simpler surface or volume elements known as primitives. The user can choose items from a menu containing such primitives, define the attributes for the primitives, enlarge, rotate, and/or translate to produce the desired final object geometry.
- Initial graphics specification (IGES)-based input : The object geometry can be generated on any commercially available CAD system that can translate the object geometry data into an IGES format which can be read in by the input module of the system. The intermediate object geometries out-putted by the expert system will be in IGES format, which can be 'retranslated' to display on the CAD system. Nearly all commercially available CAD systems provide facilities for transcribing to and from IGES data

files. This procedure is useful particularly for complex geometries where other simpler techniques cannot be employed.

- Two-dimensional graphic primitives-based input : Two-dimensional elements such as lines, arcs, etc. can also be used to define the input object geometry used by Tisza [1995]. This method is particularly useful in representing thin axis-symmetric sheet metal geometries where meridian section profiles are sufficient to define the geometry.
- Alphanumeric input: This method involves the description of the geometry in alphanumeric terms. Scheme provides much more a priori information to the knowledge-based system than any other input scheme. It identifies the orientation of line segments (horizontal, vertical, tapered, tapered-reduced), the nature of arc elements (convex, concave, convex-reduced, or concave-reduced), and the features they represent (flange, wall etc.). Such detailed information results in quantifiable savings in computational time. Since the knowledge -based system does not have to do the task of identifying the geometric primitives and recognizing the features. This scheme has been successfully used by Sitaraman et al. [1991].









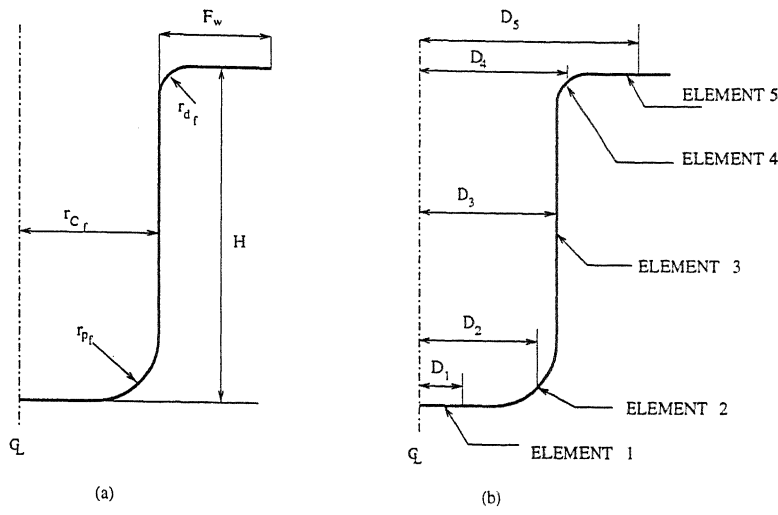
Element geometry	Conventional name
	Horizontal
	Vertical
	Tapered
	Tapered - reduced
	Convex
	Convex - reduced
	Concave
	Conave - reduced

Figure 2.2: Element library



(a) Cup Dimensions

(b) Distance to Element:

Figure 2.3: Cross section of an axisymmetric cup

For element 2:

$$P_2 = 2\pi D_2 = 2\pi(r_{cf} - r_{bf} + \frac{2r_{bf}}{\pi}), \quad L_2 = \frac{r_{bf}\pi}{2}$$

For element 3:

$$P_3 = 2\pi D_3 = 2\pi r_{cf}, \quad L_3 = H - r_{df} - r_{bf}$$

For element 4:

$$P_4 = 2\pi D_4 = 2\pi(r_{cf} + r_{df} - \frac{2r_{df}}{\pi}), \quad L_4 = \frac{r_{df}\pi}{2}$$

For element 5:

$$P_5 = 2\pi D_5 = 2\pi(r_{cf} + r_{df} + \frac{F_w - r_{df}}{2}), \quad L_5 = F_w - r_{df}$$

Sum the product of paths of the center of gravity and element lengths results in the surface area (SA) of the cup under consideration which is given by

$$SA = P_1L_1 + P_2L_2 + P_3L_3 + P_4L_4 + P_5L_5$$

To account for any possible directionality in the material properties, surface area calculated above is multiplied by 1.15 in order to obtain the required blank area with proper clearance for trimming. Thus the initial blank diameter is given by

$$D_0 = \sqrt{\frac{4SA(1.15)}{\pi}}. \quad (2.1)$$

Blank size calculated R_0 using Pappus's second theorem is input to the system.

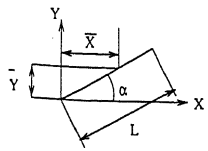
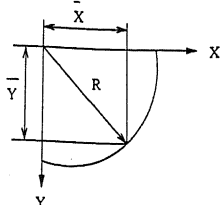
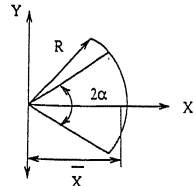
Element	Dimensions	\bar{X}	\bar{Y}	Length
Line		$\frac{L}{2} \cos \alpha$	$\frac{L}{2} \sin \alpha$	L
Quarter Circular Arc		$\frac{2R}{\pi}$	$\frac{2R}{\pi}$	$\frac{\pi}{2} R$
Circular Arc		$\frac{R \sin \alpha}{\alpha}$	—	$R \alpha$

Figure 2.4: Table of possible elements

2.3 Elementary Design Rules

In designing a die to work satisfactorily, one has to consider a number of variables which readily control the performance of the die. While designing the die and punch, the variables that affect the success and failure of a deep drawing operation are punch corner radius, die radius and punch-to-die clearance. In the present work, following rules are used to select the punch corner radius, die radius and die clearance.

Punch Corner Radius

There is no set rule for the provision of corner radius on the punch but it is customary to provide a radius of 4 to 10 times the blank thickness [ASM Handbook, 1992]. Too small a corner radius results in the excessive thinning and tearing of the bottom of cup. Ideally, the punch radius should be the same as the corner radius of the required cup because it takes its form. It is not possible in deep drawing to obtain the final cup size in a single drawing operation. Depending on the geometry of the cup, it can be necessary to for more number of drawing operations. For the initial draws, larger punch radii are used and for the final draw the requisite radius on the punch is used. Present system takes punch corner radius 3 mm larger than the final punch corner radius for all

draws. In the final draw, we get the desired punch radius.

Die Radius [Lange, 1985]

The die radius on the die does not contribute to the shape of cup during deep drawing, hence it can be made as large as possible. Higher the radius, greater the freedom for the metal to flow. Higher die radius causes the metal to be released early by the blank holder and thus lead to edge wrinkling. Too small a radius causes the thinning and tearing of the side walls of the cups. The die radius should be related to the sheet thickness by the following expression for the first draw:

$$r_d = (5 - 10) \times t_0$$

The die radius should be reduced for each subsequent redraw. It has been found to be in good practice to reduce the die radius by a factor of 0.6 to 0.8 from previous draw. Present system uses a reduction factor of 0.8 for each passes.

Die Clearance

The selection of punch-to-die clearance depends on the requirements of the drawn part and on the work metal. Ideally, the clearance between punch and die should be same as the blank thickness. Because there is decrease and then a gradual increase in the thickness of the metal as it is drawn over the die radius, clearance of about 7 to 15% greater than blank thickness (1.07 to $1.15 t_0$) helps in preventing burnishing of the side wall and punching out of the cup bottom.

The drawing force is minimal when the clearance per side is 15 to 20% greater than the stock thickness ($1.15 t_0$ to $1.20 t_0$) and the cupped portions of the part are not in contact with the walls of the punch and die.

Redrawing operation require greater clearance than the first draw in order to compensate for the increase in metal thickness during cupping. Table 2.1 lists clearances for cupping, redrawing, and sizing draws of cylindrical parts from metal of various thicknesses.

2.4 Databases

Database technology is important for the electronically integrating the various manufacturing functions of design and production. According to Martin(1975), "A database may be defined as a collection of interrelated data stored together without harmful or unnecessary redundancy to serve one or more applications in an optimal fashion; the data are stored so that they are independent of programs which use the data; a common and controlled approach is used in

Blank thickness(mm)	First Draws	Redraws	Sizing draw
Up to 0.38	1.07-1.09 t_0	1.08-1.10 t_0	1.04-1.05 t_0
0.41-1.27	1.08-1.10 t_0	1.09-1.12 t_0	1.05-1.06 t_0
1.29-3.18	1.10-1.12 t_0	1.12-1.14 t_0	1.07-1.09 t_0
3.2 and up	1.12-1.14 t_0	1.15-1.20 t_0	1.08-1.10 t_0

Table 2.1: Punch to die clearance for drawing operations, ASM Handbook [1992]

adding new data and in modifying and retrieving existing data within the database.” The database of present knowledge based system basically contains the material properties, friction coefficient, press data, as well as design rules at each stages.

2.4.1 Material Properties

The material database module contains material property information in a relational form. The stress-strain relation of sheet metal is assumed to follow the form $\bar{\sigma}_e = K(\bar{\epsilon})^n$. It consists of commonly deep drawing materials. However, the material database can be expanded to include new materials without any modifications to any other module.

Alloy	Yield Strength (MPa)	Ultimate Strength (MPa)	Constant K (MPa)	Normal Anisotropy (\bar{R})	Strain Hardening Exponent (n)
AA 3003	41	110.3	157.1	0.8	0.235
SAE 1006	200	310	617	1.4	0.310
CA-DDQ	155	330	610	2.1	0.263
BA-DDQ	157	338	612	1.76	0.248
DQ killed	172	300	610	1.6	0.220

Table 2.2: Alloy types: AA 3003 aluminum alloy, others are steel alloys, DDQ-deep drawing quality; CA-continuous annealing; BA-batch annealing

2.4.2 Tribological Data

Lubricants are essential for the success of a drawing operation as it reduces friction in the blank-holder region. If the friction forces in the blank holder region are not controlled through proper application of lubricant, the radial forces will be increased and lead to the fracture in

cup. In general lubricants used in the deep drawing operation are of two types namely oil based and water based. The final selection of lubrication largely depends upon the severity of the forming operation. Table 2.3 suggests the lubricants commonly used for a given material.

Alloy	μ	Suggested lubricant
Stainless Steel	0.05 - 0.1	EP- MO; EP-MO-EM; PC
Al Alloys	0.05 - 0.1	FA-M; FO

Table 2.3: Hyphenation indicates that several components are used in the lubricant. EM - emulsion (the listed lubricants are emulsified and 1-20% dispersed in water); EP - extreme pressure compounds (containing S,Cl and / or P); FA - fatty acids, alcohols amines and esters; MO - mineral oil; PC - polymer coating

In the deep drawing there is a sliding contact between the die surface and the work metal. The value of coefficient of friction (μ) lies between 0.05 to 0.10 [Schuler,1998]. In the present analysis, to be on the conservative side, the value of coefficient of friction is taken as $\mu = 0.10$.

2.4.3 Presses

The classification of presses for all purposes is rather difficult because of the availability of different sizes and types. However, a type and size of press for a particular job can be readily found. while selecting the type of press to use for a given job, a number of factors must be considered, namely the type of operation to be performed, part size, forced required and cycle time. Generally presses can be classified by one or more combination of the following characteristics: frame type, method of actuation of slides, number of slides and bed type.

Presses	Tonnage (Tons)
Gap frame presses	22 - 400
Single action hydraulic presses	15 - 150
Double action hydraulic presses	100 - 1000
Straight sided single action presses	200 - 1000

Table 2.4: Alloy types: AA 3003 aluminum alloy, others are steel alloys, DDQ-deep drawing quality; CA-continuous annealing; BA-batch annealing

The frame is the supporting member of the press. Power press frames can be broadly classified into two general types as gap frame and straight sided. The gap frame is the most

economical for low tonnage (1 to 250 tons) but it is not the most rigid construction. The gap frame is generally used for shallow drawing of small parts or for secondary operations. Straight sided frames are characterized by their high tonnage (up to 4000 tons in capacity) large bed size and high rigidity. In the all power presses the work is performed by the slide or ram, by means of reciprocating motion to and from the press bed. The drive is the type of mechanism used to obtain ram movement. The two general categories of drives are mechanical and hydraulic. Some of the mechanical drives include crankshaft, eccentric and cam. Hydraulic drives obtain ram movement by pumping incompressible fluid into a cylinder with a closed end reacting against a piston to move the slide. Hydraulic presses have the advantage of being able to exert their full tonnage at any point in the stroke and can have any shut height within the maximum piston stroke. On the other hand, mechanical presses can only exert its maximum tonnage at the end of the stroke. Mechanical presses have a faster cycle time and more positive displacement control and are better suited for mass production of simple shapes.

The action or number of slides or rams on a press can either be single, double or triple. A single action press consists of a single ram, which holds the punch steel or upper part of a die set. A double action press consists of two rams or slides, one outer and another inner. The outer slide acts as the blank holder and the inner slide continues to descend. Double action presses generally have a maximum inner ram capacity of 2000 tons and usually have longer strokes which contributes to added expense.

Table 2.4 suggests the presses commonly used for a given tonnage.

2.5 Process Analysis

The draw-ability of the sheet metal is defined by the limiting drawing ratio (LDR), which is the ratio of the maximum diameter of blank that can be drawn successfully without tearing of cup, to the punch diameter. From the critical literature review (refer Chapter 1), it is evident that the LDR depends strongly on the normal anisotropy value \bar{R} , strain hardening exponent n and die geometry. A high normal anisotropy (\bar{R}) indicates a better draw-ability (higher limiting drawing ratio), and induces a high resistance of a sheet to thinning. Thus, in order to estimate the limiting drawing ratio (LDR) for each pass, an analytical model has been developed. In the present work, limiting drawing ratio is estimated for the cylindrical cup with a flat-nosed punch using an integral technique based on the load maximum principle for localization of plastic flow. Leu[1999] also proposed the analytical model based on the same principle for first draw only. In his model, limiting drawing ratio was estimated for a given cup radius. Also, the effect of thickness on the limiting drawing ratio was not considered in his work. In the present work, thickness of the sheet is taken into account as it is one of the important process variable. The model developed in the work is used in the process sequence

design module to calculate the number of passes required to achieve the final cup diameter.

Assumptions

- The material properties are assumed to be rotationally symmetric, so that there is a planar anisotropy and normal anisotropy. Planar anisotropy is defined as the ratio of width to thickness strain. Average value of normal anisotropy is given by

$$\bar{R} = \frac{R_0 + 2R_{45^\circ} + R_{90^\circ}}{4} \quad (2.2)$$

where R_0 , R_{45° and R_{90° are the values of planar anisotropy at 0° , 45° , 90° to the rolling direction.

- Material is assumed to be rigid-plastic.
- The bending effects around the die arc, (r_d) and punch nose radius, (r_p) is neglected.
- Deformation in the flange region is assumed to be plain strain i.e., the thickness remains constant as that of initial blank. Although thinning occurs near the base and thickening occurs near the top but these changes are not considered in the present work as they are not very significant [Hosford, 1983].
- Material is assumed to be yielding according to Hill's anisotropic plasticity theory.
- The strain hardening characteristics of sheet metal is assumed to follow the form

$$\bar{\sigma}_e = K(\bar{\epsilon})^n \quad (2.3)$$

where $\bar{\sigma}_e$ is the generalized stress, $\bar{\epsilon}$ is the generalized strain, n is the strain hardening exponent and K is the material constant.

Hill's Anisotropic Yield Criterion

Using the Hill's anisotropic yield criterion, relationships of stresses and incremental strains are given by [Leu, 1999]:

$$\bar{\sigma}_e = \sqrt{\frac{1}{1 + \bar{R}}} [(\sigma_\theta - \sigma_z)^2 - (\sigma_r - \sigma_z)^2 + \bar{R}(\sigma_r - \sigma_\theta)^2]^{\frac{1}{2}} \quad (2.4)$$

$$d\bar{\epsilon} = \frac{\sqrt{1 + \bar{R}}}{1 + 2\bar{R}} [(d\epsilon_\theta - \bar{R}d\epsilon_z)^2 + (d\epsilon_r - \bar{R}d\epsilon_z)^2 + \bar{R}(d\epsilon_r - d\epsilon_\theta)^2]^{\frac{1}{2}} \quad (2.5)$$

$$\frac{d\epsilon_r}{\bar{R}(\sigma_r - \sigma_\theta) + (\sigma_r - \sigma_z)} = \frac{d\epsilon_\theta}{\bar{R}(\sigma_\theta - \sigma_r) + (\sigma_\theta - \sigma_z)} = \frac{d\epsilon_z}{(\sigma_z - \sigma_\theta) + (\sigma_z - \sigma_r)} = \frac{d\bar{\epsilon}}{(1 + \bar{R})\bar{\sigma}_e} \quad (2.6)$$

where σ_r , σ_θ and σ_z are stresses in x, y and z directions and $d\epsilon_r$, $d\epsilon_\theta$ and $d\epsilon_z$ are strain increments in the directions x, y and z.

2.5.1 Draw Analysis

Figure 2.5 shows the schematic diagram for a cup-drawing operation in which a circular blank of original radius R_0 and thickness t_0 is deep drawn by the flat-bottomed punch through a die opening of radius r_{cd} .

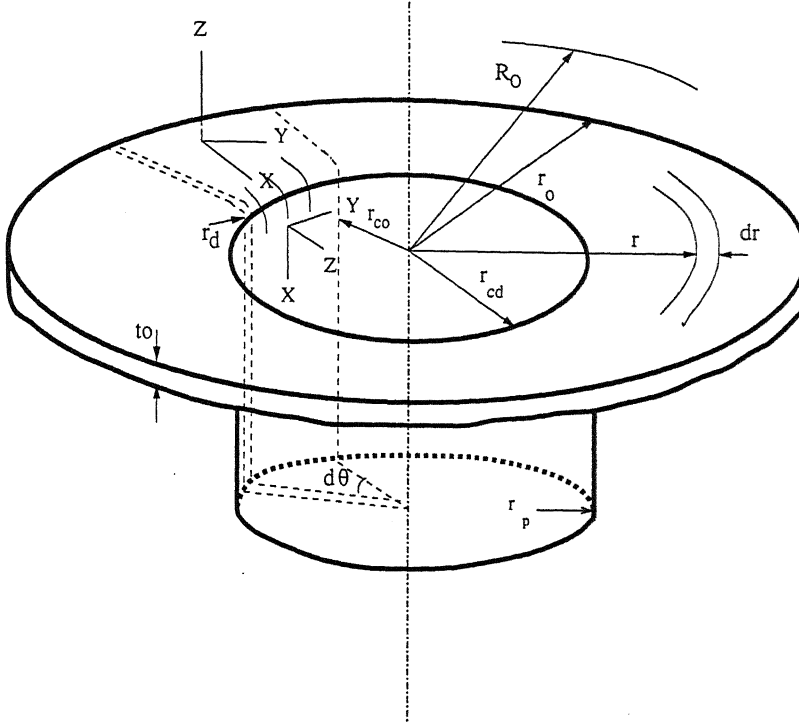


Figure 2.5: Schematic representation of cup drawing, showing the co-ordinate system and dimensional notations.

In the cup wall section, the maximum diametric reduction is usually limited by the maximum allowable drawing force at the punch nose radius (r_p). The critical drawing load P_c is obtained using a criterion based on the tensile instability in the cup wall. The critical drawing force (P_c) at a certain stage of the punch stroke is given by

$$P_c = 2\pi r_{c0} t \sigma_r \quad (2.7)$$

where t is the instantaneous thickness of the cup wall and is given by

$$t = t_0 e^{\epsilon_z} \quad (2.8)$$

and based on the plane-strain conditions, given by $d\epsilon_\theta = 0$ and $\sigma_z = 0$, and the volume constancy of plastic deformation, the drawing stress σ_r can be written as:

$$\sigma_r = \frac{K(1 + \bar{R})}{\sqrt{1 + 2\bar{R}}} \bar{\epsilon}^n \quad (2.9)$$

Critical drawing load (P_c) at the LDR can be obtained by maximizing the drawing force at the beginning of the punch nose radius in the cup wall with respect to the effective strain, i.e. $\frac{\partial P_c}{\partial \bar{\epsilon}} = 0$. From the obtained critical effective strain, the critical drawing force is obtained as:

$$P_c = 2\pi r_{c0} t_0 \left(\frac{1 + \bar{R}}{\sqrt{1 + 2\bar{R}}} \right)^{1+n} (n^n e^{-n} K) \quad (2.10)$$

In the die arc region, as the sheet metal slides along the die corner during drawing, using the force equilibrium and the increase in rope tension around a capstan and with friction between radii r_{c0} and r_{cd} as shown in the Figure 2.6 [Ghosh and Mallik, 1994], the drawing force per unit circumferential length at r_{cd} is given by

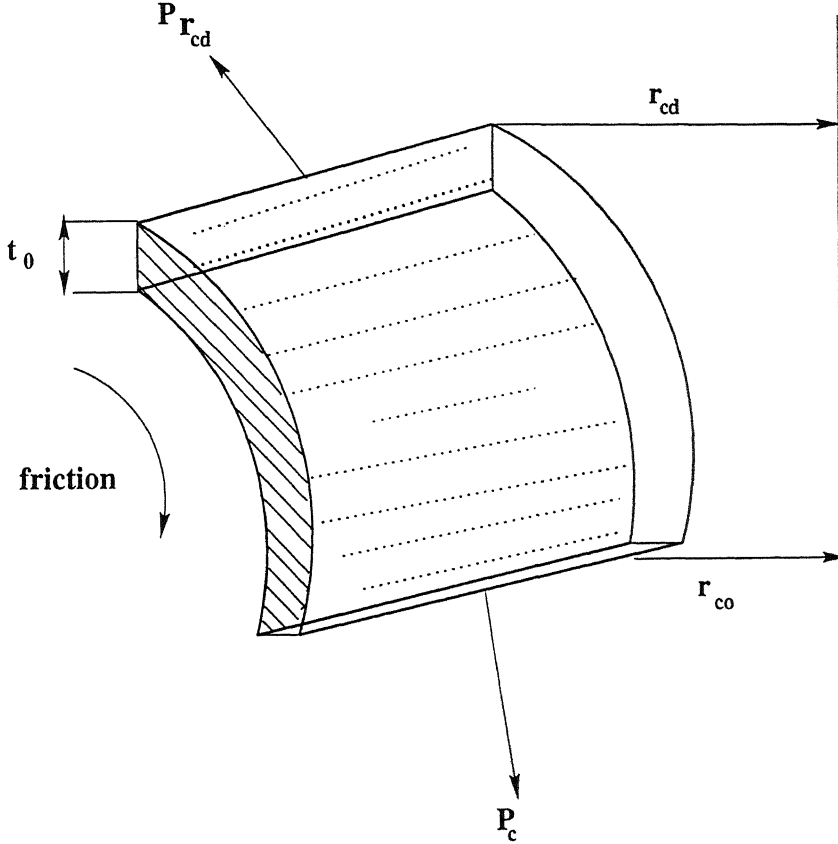


Figure 2.6: Force acting on the Die Arc Region

$$\frac{P_{r_{cd}}}{2\pi r_{cd}} = \frac{P_c}{2\pi r_{c0}} \frac{r_{c0}}{r_{cd}} e^{-\frac{\pi}{2}\mu} \quad (2.11)$$

Substituting Eq. 2.10 in the above equation, the drawing stress σ_r at r_{cd} , correlating with the condition of the critical drawing force can be obtained as

$$\sigma_{r_{cd}} = \left(\frac{1 + \bar{R}}{\sqrt{1 + 2\bar{R}}} \right)^{1+n} (n^n e^{-n} K) \left(\frac{r_{c0}}{r_{cd}} \right) e^{-\frac{\pi}{2}\mu} t_0 \quad (2.12)$$

where $\sigma_{r_{cd}}$ is the radial drawing stress at r_{cd} in the pure radial drawing of the flange region.

The stresses acting on an element in the flange region at the current radius r are shown in figure 2.7 and the equation of radial equilibrium can be written as

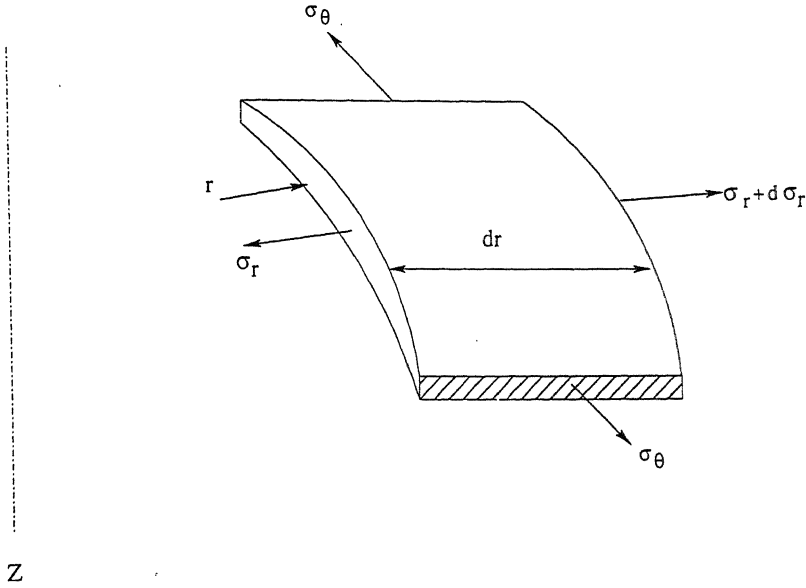


Figure 2.7: Radial stresses in the flange element

$$\frac{d\sigma_r}{dr} = -\frac{(\sigma_r - \sigma_\theta)}{r} \quad (2.13)$$

Under the plain strain deformation condition of the flange, i.e. $d\epsilon_z = 0$, the relationship of stresses σ_r and σ_θ can be obtained as

$$(\sigma_r - \sigma_\theta) = \bar{\sigma}_e \left[\frac{2(1 + \bar{R})}{2\bar{R} + 1} \right]^{1/2} \quad (2.14)$$

Substituting above equation in Eq. 2.13, and integrating the equation from r_{cd} to r_0 for the maximum radius of R_0 , the radial drawing stress at the position r_{cd} in the flange can be obtained as

$$\sigma_{r_{cd}} = \sigma_{r_0} + K \left[\sqrt{\frac{2(1 + \bar{R})}{2\bar{R} + 1}} \right]^{1+n} \int_{r_0}^{r_{cd}} \ln\left(\frac{R}{r}\right)^n \frac{dr}{r} \quad (2.15)$$

In Eq. 2.15 σ_{r_0} denotes the radial friction stress resulting from the blank holding stress at r_0 and it can be taken as $2\mu(1.1\sigma_y)\frac{R_0}{r_0}$ [Lange, 1985].

The limiting drawing ratio is determined from the condition that the drawing stress $\sigma_{r_{cd}}$ (Eq. 2.12) of the die arc region to cause plastic instability in the cup wall, is equal to the radial drawing stress $\sigma_{r_{cd}}$ of the flange region (Eq. 2.15), due to continuity of stress. Equating Eqs. 2.12 and 2.15 the resulting equation is obtained as

$$\begin{aligned}
f(LDR_0) = & -\frac{C_1}{1 + \frac{r_d}{R_0} LDR_0} + C_3 \left(\frac{1}{1 + \frac{r_d LDR_0}{R_0}} \right) \frac{LDR_0}{\sqrt{LDR_0^2 \left(\frac{1}{1 + \frac{LDR_0 r_d}{R_0}} \right)^2 - \left(\frac{R_2}{r_{cd}} \right)^2 + 1}} \\
& + C_2(1+n) \ln \left(\sqrt{LDR_0^2 \left(\frac{1}{1 + \frac{LDR_0 r_d}{R_0}} \right)^2 - \left(\frac{R_2}{r_{cd}} \right)^2 + 1} \right) \\
& - 2nC_2 \ln \left(LDR_0 \left(\frac{1}{1 + \frac{LDR_0 r_d}{R_0}} \right) + \sqrt{LDR_0^2 \left(\frac{1}{1 + \frac{LDR_0 r_d}{R_0}} \right)^2 - \left(\frac{R_2}{r_{cd}} \right)^2 + 1} \right) \\
& - 2nC_2 \left[\frac{1}{1 + \frac{LDR_0 r_d}{R_0} \frac{LDR_0}{\sqrt{LDR_0^2 \left(\frac{1}{1 + \frac{LDR_0 r_d}{R_0}} \right)^2 - \left(\frac{R_2}{r_{cd}} \right)^2 + 1}}} \right] \\
& + 2nC_2 \left[\ln \left(\frac{R_2}{r_{cd}} + 1 \right) + \frac{1}{\frac{R_2}{r_{cd}} + 1} \right] = 0 \tag{2.16}
\end{aligned}$$

where the $\frac{R_2}{r_{cd}}$ can be evaluated by the volume constancy of plastic deformation in the die arc region. Equating the volume of metal before and during radial drawing (Figure 2.8), one can get

$$\pi(R_2^2 - R_1^2)t_0 = 2\pi\left(r_{cd} - \frac{2r_d}{\pi}\right)\left(\pi r_d \frac{t_0}{2}\right)$$

and it can be written as

$$\frac{R_2}{r_{cd}} = \left[\pi \left(\frac{r_d}{\frac{R_0}{LDR_0} + r_d} - \frac{2r_d^2}{\pi \left(\frac{R_0}{LDR_0} + r_d \right)^2} \right) + \left(\frac{1}{1 + \frac{LDR_0 r_d}{R_0}} \right)^2 \left(\frac{R_1}{r_{c0}} \right)^2 \right]^{\frac{1}{2}} \tag{2.17}$$

$\frac{R_1}{r_{c0}}$ can be determined from the condition that the effective strain in the flange never exceeds the critical strain in the cup wall.

Thus Eq. 2.16 derived above is a function of the LDR in terms of initial blank thickness t_0 , normal anisotropy \bar{R} , strain hardening exponent n , coefficient of friction μ , die arc radius r_d , initial blank radius R_0 and yield strength σ_y . This non-linear equation in terms of LDR can be solved by using Newton-Raphson Method.

Often it is not possible to obtain the desired reduction in the first draw. Redrawing once or several times may be necessary. The characteristics of redrawing can be described using the same variables as found in the first draw operation. A cup just prior to the start of metal

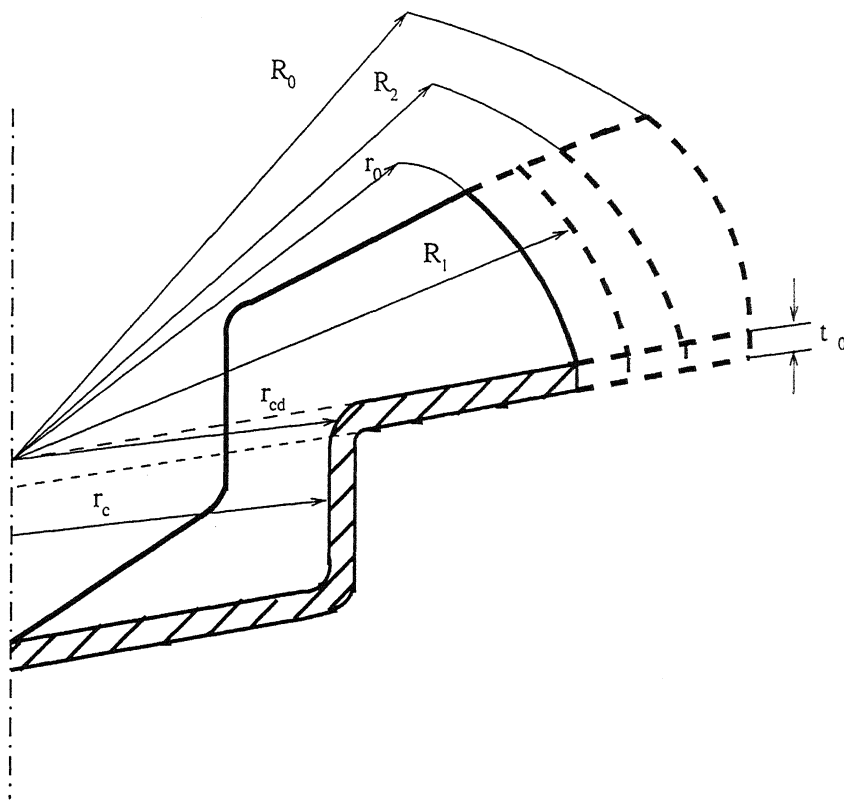
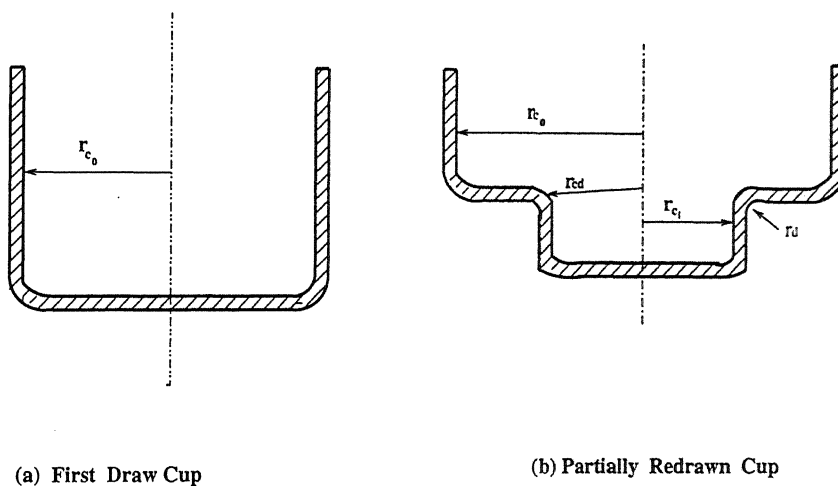


Figure 2.8: Section of a partial drawn cup



(a) First Draw Cup

(b) Partially Redrawn Cup

Figure 2.9: Redrawing of Cups

flow in the redraw die is illustrated in Figure 2.9 a. Redrawing, like cupping (first draw) is also characterized by the limiting reduction. During the first draw, strain hardening at the top of the cup wall is maximum and it goes on decreasing as we move towards the bottom of cup. The extent of strain hardening is determined by the amount of reduction achieved. The strain hardening in the cup is given by the condition that $\bar{\epsilon}$ is never more than about 3%

greater than the numerical value of hoop strain induced during pure radial drawing [Johnson and Mellor, 1972]. So the strain induced in the different passes is given by

$$\bar{\epsilon}^{i-1} = \ln \left(\frac{r_{c_{i-1}}}{r_{c_i}} \right) = \ln (LDR_i) \quad (2.18)$$

Where i denotes the number of draws and is given by $i = 1, 2, 3, \dots, N$.

During a redraw operation, the punch which is smaller in diameter than the previous draw punch, contacts the bottom of the which was produced in the previous drawing operation. Unlike the cup wall and flange, the cup bottom has not seen any deformation in the prior draws, hence the yield strength can be presumed to be the same as that of initial material. Therefore, criterion for the plastic instability in the cup wall used in the first draw can be applied here. Maximizing the drawing force P with respect to the effective strain $\bar{\epsilon}$. Critical drawing load P_{c_2} at the onset of necking can be obtained. Material flows along the die arc region in the similar way as happened in the first draw.

The annular portion of the sheet metal workpiece (see fig 2.7) between the blank-holder and die is subjected to a pure radial drawing. The effective strain $\bar{\epsilon}$ in the flange region is obtained by adding the strain induced in the cup wall due to the previous draws.

One can obtain the radial stress as

$$d\sigma_r^{II} = -K \left[\ln(LDR_i) + \sqrt{\frac{2(1+\bar{R})}{1+2\bar{R}}} \ln\left(\frac{R}{r}\right) \right]^n \sqrt{\frac{2(1+\bar{R})}{1+2\bar{R}}} \frac{dr}{r} \quad (2.19)$$

Redrawing can be considered as the steady state process as the material is drawn inward with the continuous supply from cup wall formed during the earlier draw [Hosford, 1983]. Integrating the above equation from r_{cd} to the maximum radius $r_{c_{i-1}}$ formed during earlier draw,

$$\int_{r_{cd}}^{r_{c_{i-1}}} d\sigma_r^{II} = \int_{r_{cd}}^{r_{c_{i-1}}} -K \left[\ln(LDR_{i-1}) + \sqrt{\frac{2(1+\bar{R})}{1+2\bar{R}}} \ln\left(\frac{R}{r}\right) \right]^n \sqrt{\frac{2(1+\bar{R})}{1+2\bar{R}}} \frac{dr}{r}$$

Expanding using Binomial theorem and neglecting higher order terms, one can get

$$\sigma_r^{II} = \sigma_{r_{i-1}}^{II} + K \sqrt{\frac{2(1+\bar{R})}{1+2\bar{R}}} [\ln(LDR_{i-1})]^n \int_{r_{cd}}^{r_{c_{i-1}}} \left[1 + \frac{n \sqrt{\frac{2(1+\bar{R})}{1+2\bar{R}}}}{\ln(LDR_{i-1})} \ln\left(\frac{R}{r}\right) \right] \frac{dr}{r}$$

The limiting drawing ratio is determined from the condition that the drawing stress in the cup wall is equal to the radial drawing stress of the flange region, due to continuity of stress.

$$f(LDR_i) = -\frac{C_1 r_{c_{i-1}}}{r_{c_{i-1}} + LDR_{i-1} r_d} + C_3 \frac{r_{c_{i-1}}}{r_d + r_{c_{i-1}}/LDR_i} + C_4 \ln \left(\frac{r_{c_{i-1}}}{r_d + r_{c_{i-1}}/LDR_i} \right) +$$

$$\begin{aligned}
C_5 & \left[\ln \left(\frac{r_{c_{i-1}}}{r_d + r_{c_{i-1}}/LDR_i} \right) - \frac{1}{(r_d + r_{c_{i-1}}/LDR_i)^2 ((R_{i+1}/r_{cd})^2 - 1)} \right] \\
& r_{c_{i-1}} \sqrt{(r_d + r_{c_{i-1}}/LDR_i)^2 ((R_{i+1}/r_{cd})^2 - 1) + r_{c_{i-1}}^2 -} \\
& (r_d + r_{c_{i-1}}/LDR_i)^2 (R_{i+1}/r_{cd}) - (r_{c_{i-1}}^2 - (r_d + r_{c_{i-1}}/LDR_i)^2) \Big] \\
& + C_5 \ln \left(r_{c_{i-1}} + \sqrt{(r_d + r_{c_{i-1}}/LDR_i)^2 ((R_{i+1}/r_{cd})^2 - 1) + r_{c_{i-1}}^2} \right) \\
& - C_5 \ln \left((r_d + r_{c_{i-1}}/LDR_i) (1 + R_{i+1}/r_{cd}) \right) \tag{2.20}
\end{aligned}$$

where,

$$\begin{aligned}
C_4 &= K \sqrt{\frac{2(1 + \bar{R})}{1 + 2\bar{R}}} [\ln(LDR_{i-1})]^n \\
C_5 &= 2Kn \frac{2(1 + \bar{R})}{1 + 2\bar{R}} [\ln(LDR_{i-1})]^{n-1}
\end{aligned}$$

$$LDR_i = \frac{r_{c_{i-1}}}{r_{c_i}}$$

$$r_{cd} = r_{c_i} + r_d$$

The constants C_1 and C_3 remains same as in the first draw analysis.

$\frac{R_{i+1}}{r_{cd}}$ can be obtained by considering the volume constancy of plastic deformation in the die arc region.

In the multiple passes, strain hardening caused during each pass should be taken into account for the subsequent passes. Eq.2.16 can be used to estimate the limiting drawing ratio after the cup has been annealed since the stain induced in the cup would be zero and the bottom of the cup can be considered as the initial blank.

Chapter 3

System Implementation

3.1 Introduction

A Knowledge based system is implemented for designing and process planning of axisymmetric deep drawn components. The system involves the following steps to achieve the final result:

- Geometry Design: Parametric designing of the object geometry.
- Database : Selecting the required material properties, friction coefficient etc. from the database.
- Process sequencing: Generating the feasible process plans considering the analytical model and design rules.

This system is implemented using VC++ 6.0, Windows 98.

The main window is a simple menu-based front-end to the various modules, as shown in Figure 3.1. The main window starts with the execution of the system. It consists of the installed module blocks in the menu bar. By selecting the menu items individual modules can be activated.

3.2 Object Modeling

The input to system is the final object. Generally, the format of input to CAPP system can be either in a text or graphic input. Text input is also referred to as interactive input, where a number of data are entered through the keyboard. Graphic input also referred as interface input, where the geometrical details of the part model are entered from a given drawing details using predefined geometric primitives.

In the present system both text and graphical types of input have been adopted. Interactive input is adopted for design data entry and the drawing details of the shape are entered through graphical input interface using VC++ 6.0. The implementation is carried out from

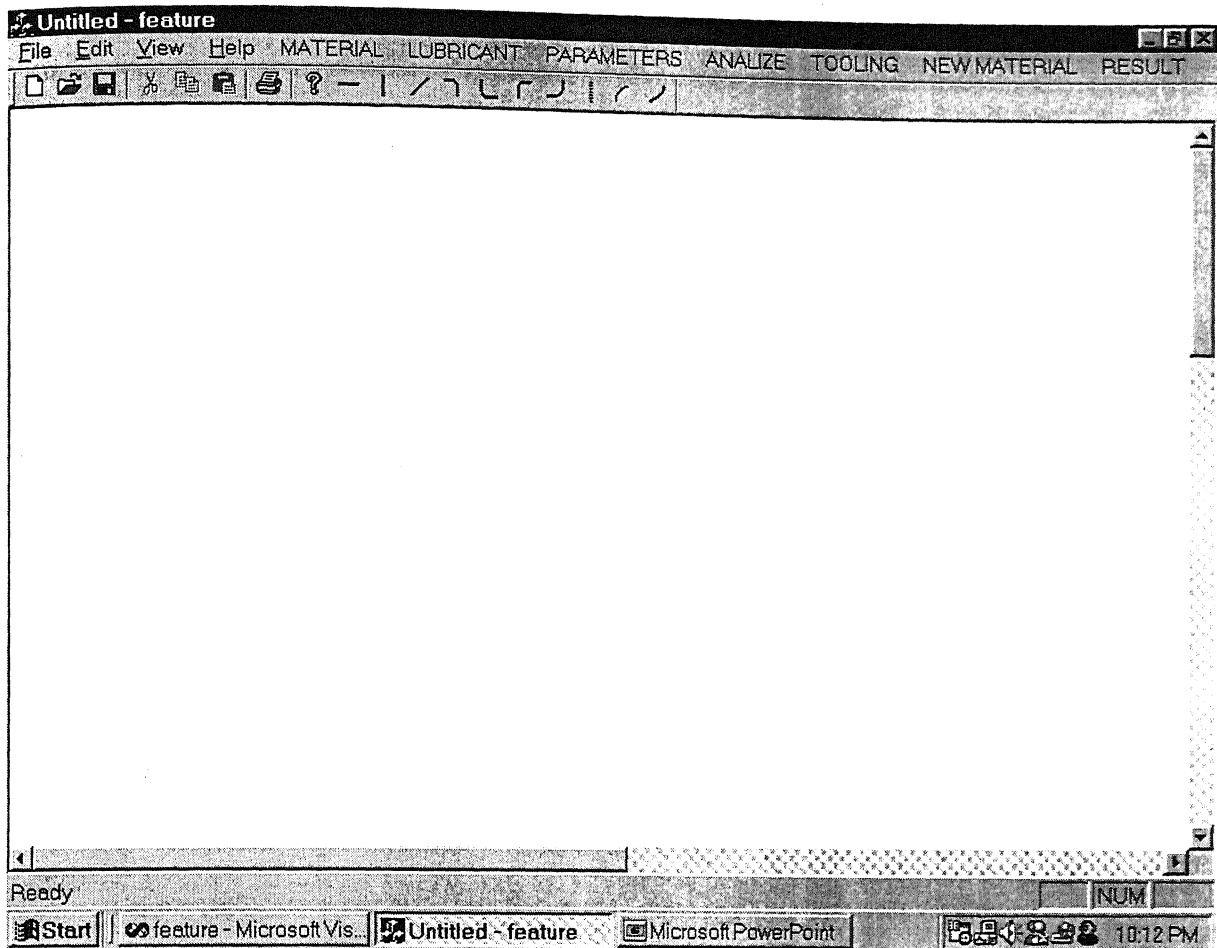


Figure 3.1: Main window

bottom to the top of the cup. The final part geometry, which is input to the system, is concatenation of the two-dimensional elements such as lines, arcs, etc. First of all, the axis of symmetry is defined and with respect to the axis of symmetry the final part geometry is modeled using the graphic primitives. Parametric modeling of object geometry is done, as shown in Figure 3.2. For concatenation, the end coordinates of each feature primitive becomes the start coordinate of next primitive. Pappus's Second Theorem is used to calculate the surface area of the component created. Designing the arc elements related to die and punch uses the empirical relations presented in Section 2.2. Identification of the nature of arc elements (convex, concave, convex-reduced, or concave-reduced), and the features they represent (die arc and punch arc) makes the designing of die and punch easier.

3.3 Databases

The database of this implemented system is basically an independent part containing the material properties, frictional data, press data, as well as design rules. The database of the

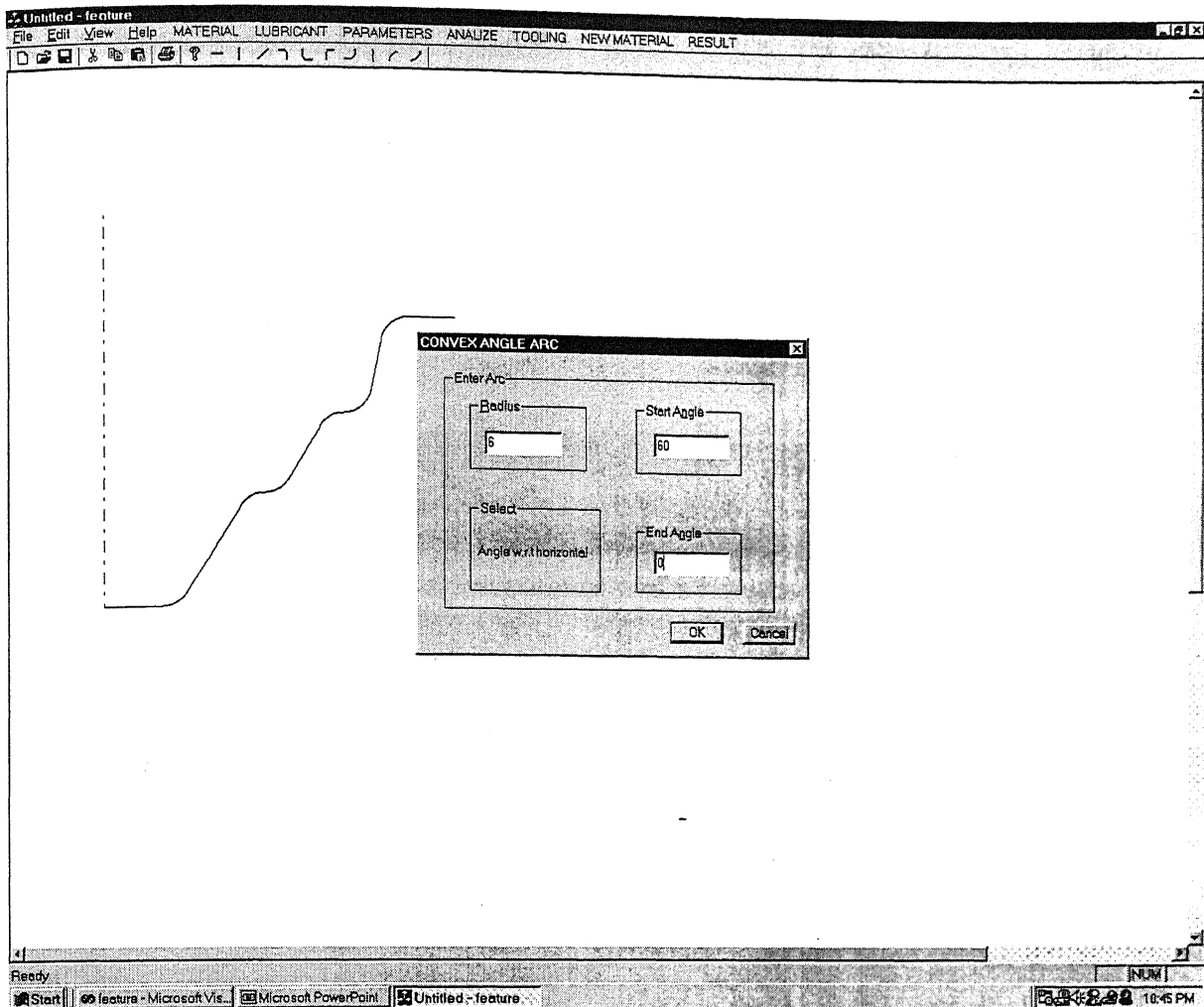


Figure 3.2: Object modeling

system designed to be flexible with an easily extendable structure. Database can be modified with recompiling the system for effective database management.

3.3.1 Selection of Material

The material database module contains material properties of commonly deep drawn materials. However, the material database can be expanded to include new materials without any modifications to any other module. The material database is activated from the MATERIAL menu, as shown in Figure 3.3. The user can give new material by selecting the NEW MATERIAL menu from the main window.

3.3.2 Selection of Lubricant

Different lubricants are used for deep drawing of different materials. The present system provides a set of lubricants commonly used in deep drawing. In, deep drawing there is a

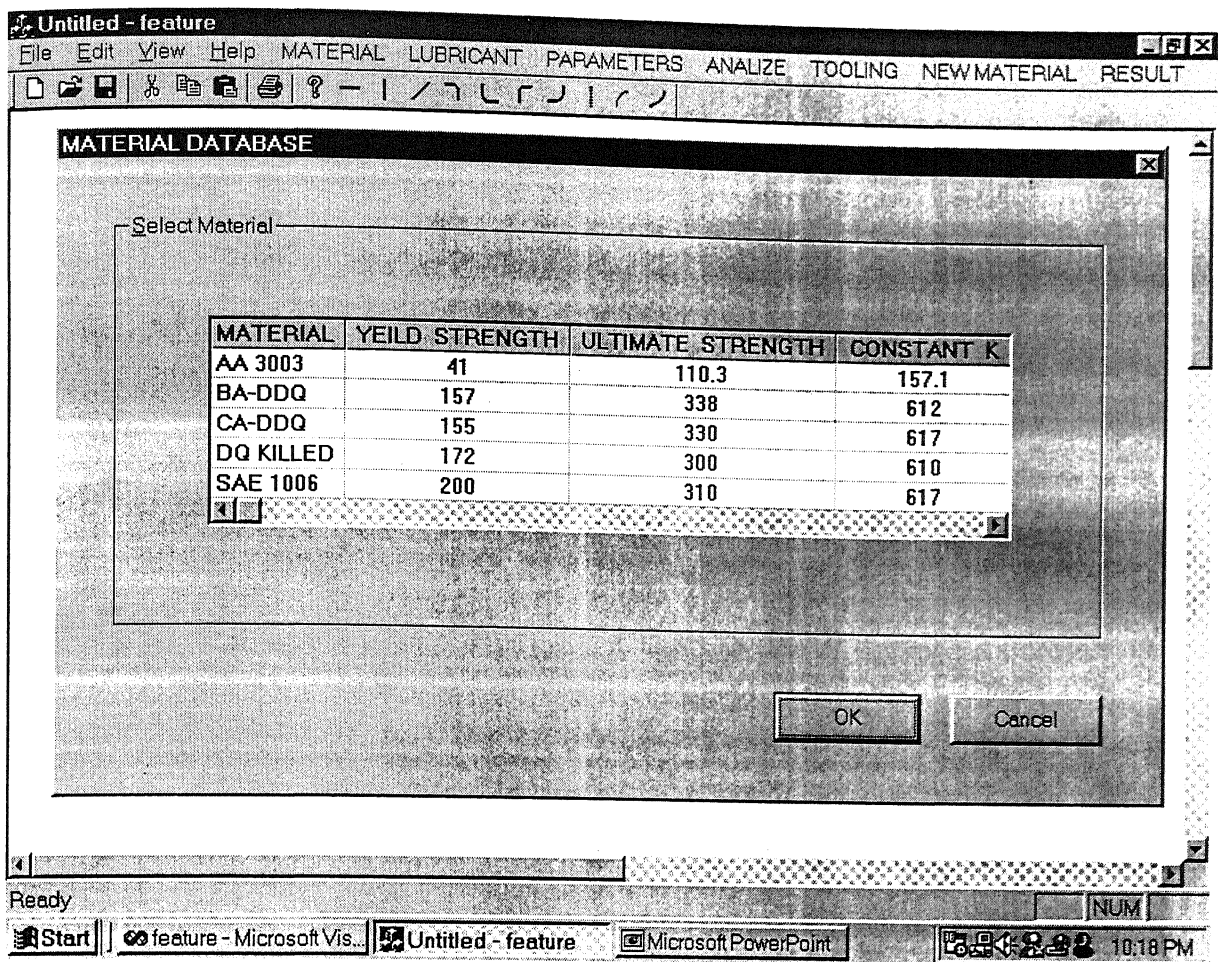


Figure 3.3: Material database

sliding contact between the die surface and work metal. The value of coefficient of friction (μ) lies between 0.05 to 0.10 [Schuler,1998]. In the present analysis, to be on conservative side, the value of coefficient of friction is taken as $\mu = 0.10$.

3.3.3 Selection of Press

The press database contains the tonnage available with a set of presses commonly used in deep drawing. The user can select the press considering the drawing force required.

3.4 Process Sequence Design Module

Present Knowledge based system is implemented to generate the process plan to achieve the final cup diameter. This is done using the process sequence design module. Process sequence design module is the backbone of the present Knowledge based system. Since the Eq.2.20 presented in Chapter 2 gives more general expression for LDR for the redrawing operation; hence it has been incorporated in the process analysis module. It estimates the limiting

drawing ratio for the first stage as well for the subsequent passes. By calculating the limiting drawing ratio at each pass one can know that how many number of draws are required to achieve the final cup geometry. For the components having large height as compared to the diameter, desired cup height and diameter may not be obtainable with one redraw. Several redraws are carried out successively. But the progressive strain hardening of the material determines the need for annealing. The term 'total drawing ratio' can be used to determine at which stage annealing is required. The total drawing ratio DR_{total} is equal to the product of LDR of all draws. For a given material if this limit is reached, then the alternative plans are generated by performing annealing at different stages. Flow chart in Figure 3.4 shows the working of process sequence design module.

In the process planning, the type of operations and possible sequence of them should be determined including the necessary intermediate heat treatments as well. This is very part of the whole design process where the human knowledge and expertise has a decisive role. The key issue in the process planning is the selection of appropriate operations to determine their optimum sequence. There is obviously more than one possible solution for the production of a given component. The system is capable to offer alternate solutions. From the various alternatives offered by system, the optimum one may be selected according to the optimization criteria stated by user (eg. the necessary number of drawing operation, necessity of intermediate heat- treatments, etc.).

3.5 Viewing the Results

The results of the technological process planning can be displayed by selecting the RESULT menu from the main window. The process plan generated is displayed on the main window.

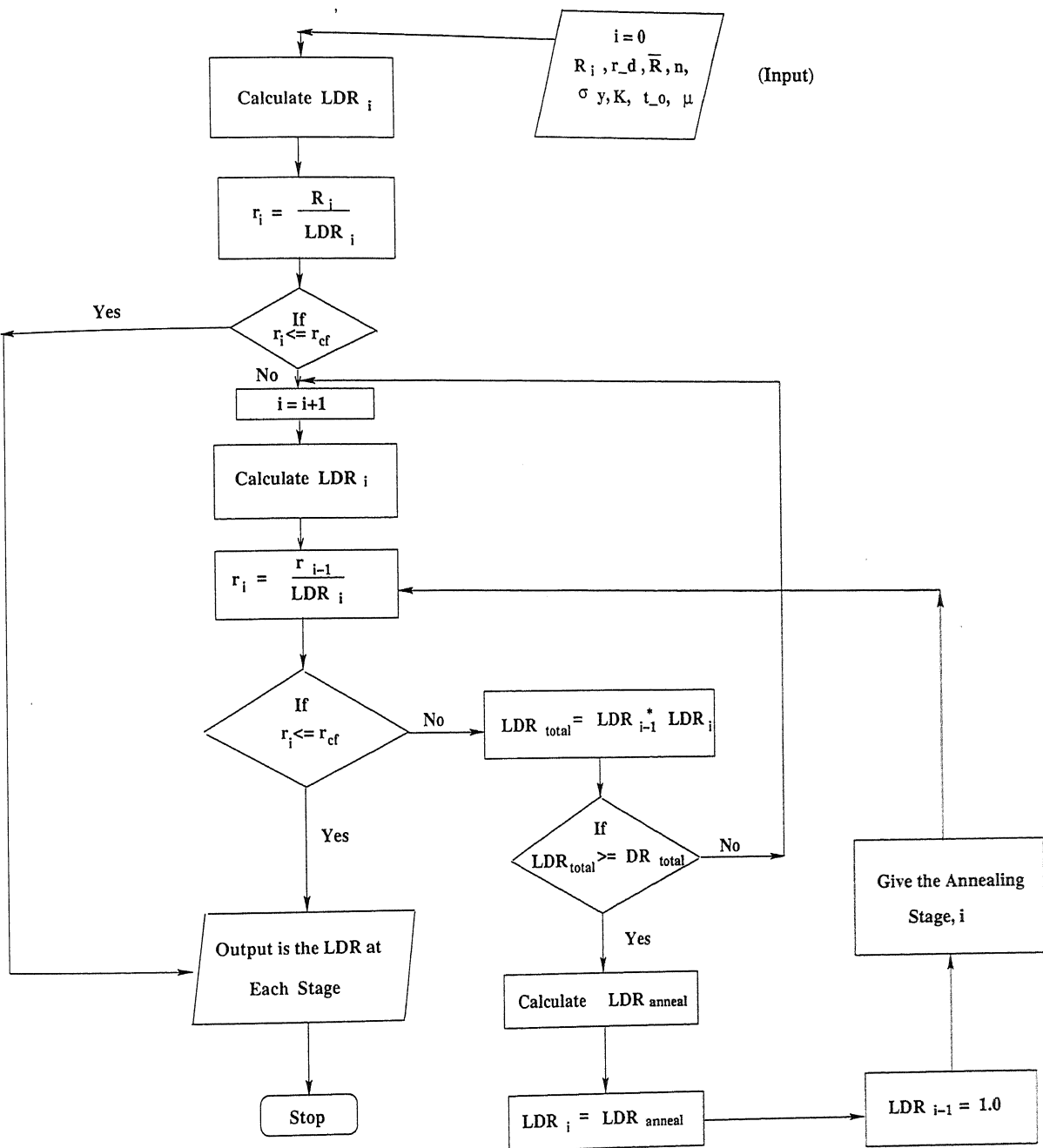


Figure 3.4: Process Sequence Design Flow Chart

Chapter 4

Results and Discussion

4.1 Introduction

The analytical model developed by Sonis[2001] to predict the LDR is used in the present system. Its predictions are compared with the available experimental results and are presented in section 4.2. The results from the developed system are presented in the section 4.3. In the present system, the product geometry selected for the various cases are in such a way that its capabilities can be demonstrated. In the end, the procedural steps are shown for a case to obtain the output from the developed system.

4.2 Validation

First Draw

Limiting drawing ratios predicted by the model presented by Sonis[2001] are compared with the available experimental results of Whiteley[1960] and Rogers and Anderson[1971] and are presented in Figures 4.1 and 4.2 respectively.

Figure 4.1 shows the comparison between the predictions of the model presented by Sonis[2001] with the experimental result of Whiteley[1960] for aluminum. It can be seen from the fig. 4.1 that the predictions of the present model and the experimental results of Whiteley[1960] are in good agreement. The data regarding the stress-strain relationship of the material, die geometry and lubricant used are not reported. Therefore limiting drawing ratio from the present model are estimated by using the guidelines for die design given in the handbooks [Lange, 1985 and Schuler, 1998], while the stress-strain characteristics are taken from El-Sebaie and Mellor [1972]. In general, die radius depends on the thickness of the sheet metal used and it varies from 5-10 times of sheet thickness [Lange, 1985]. Also, in the deep drawing the coefficient of friction usually varies from 0.05 to 0.10 [Schuler, 1998]. Final cup diameter and initial blank thickness is taken as 4 inch and 0.040 inch respectively [Rogers and Anderson, 1971]. Material properties used for aluminum are [El-Sebaie and Mellor, 1972]

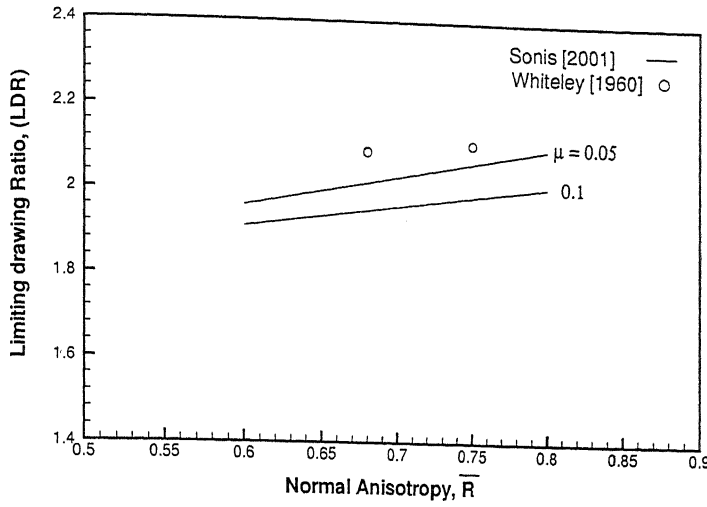


Figure 4.1: Variation of LDR with normal anisotropic value for flat bottom cups drawn from soft Aluminum. ($\bar{\sigma}_e = 118(\bar{\epsilon}_e)^{0.227}$ MPa, $\sigma_y = 28.8$ MPa, $r_{cf} = 50.8$ mm, $r_d = 8.635$ mm, $t_0 = 1.016$ mm)

taken as:

$$\text{Generalized stress } (\bar{\sigma}) = 118(\bar{\epsilon})^{0.227} \text{ MPa.}$$

$$\text{Yield Strength } (\sigma_y) = 28.8 \text{ MPa}$$

However, the slight discrepancy in the predictions of the present model and the experimental results of Whiteley [1960] can be attributed to the possible variations in the stress-strain relationship, different friction condition and tool geometry used in the experiment.

Figure 4.2 shows the comparison between the predictions of the model presented by Sonis [2001] with the experimental result of Rogers and Anderson [1971] for AA 3003 material. It can be seen from the Figure 4.2 that the predictions of the present model and the experimental results of Rogers and Anderson [1971] are in good agreement. They carried out experiments by drawing 4 inch diameter flat bottom cups from the blanks of various diameters of 0.040 inch thick sheets. For the above experiment [Rogers and Anderson, 1971], no information regarding the material properties, die geometry and lubricant used are reported, therefore the predictions of the present model are estimated by choosing die radius r_d equal to 8.5 times sheet metal thickness [Lange, 1985] and the coefficient of friction ranging from 0.05 to 0.10 [Schuler, 1998]. Results are compared for both the friction conditions i.e. at $\mu = 0.05$ and $\mu = 0.10$. Material properties of AA 3003 are given as [ASM Handbook, 1992]:

$$\text{Generalized stress } (\bar{\sigma}) = 157.1(\bar{\epsilon})^{0.235} \text{ MPa. Yield Strength } (\sigma_y) = 41 \text{ MPa}$$

The discrepancy between the results of Rogers and Anderson [1971] presented in Figure 4.2 can be attributed to the possible variations in the stress-strain relationships, friction

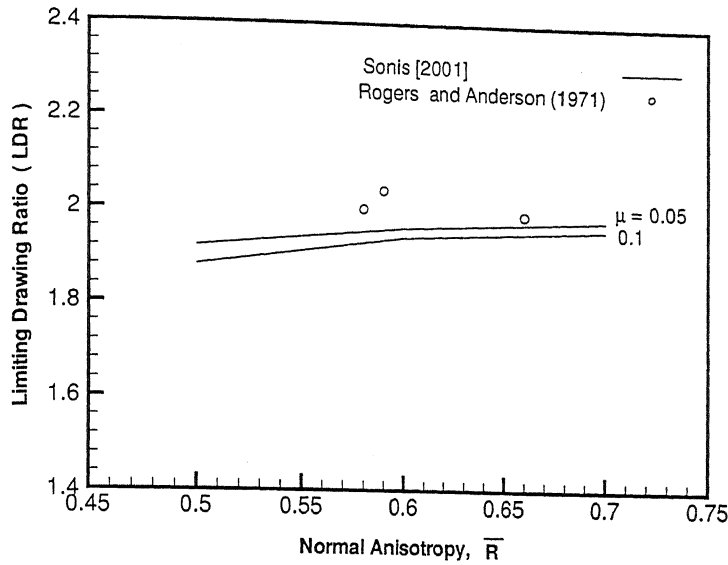


Figure 4.2: Variation of LDR with normal anisotropic value for flat bottom cups drawn from AA 3003. ($\bar{\sigma}_e = 157.1(\bar{\epsilon}_e)^{0.235}$ MPa, $\sigma_y = 41$ MPa, $r_{cf} = 50.8$ mm, $r_d = 8.635$ mm, $t_0 = 1.016$ mm)

Material type	t_0 (mm)	K (MPa)	σ_y (MPa)	\bar{R}	n	LDR (Present)	LDR (exp.)	Δ LDR
SAE 1006	1.0	617	200	1.0	0.31	2.06	2.10	-0.04
SAE 1006	1.0	617	200	1.25	0.31	2.15	2.22	-0.07
SAE 1006	1.0	617	200	1.5	0.31	2.23	2.24	-0.01

Table 4.1: Comparison of experimental data and predictions of the model presented by Sonis[2001] for mild steel sheets. ($\bar{\sigma}_e = 617(\bar{\epsilon}_e)^{0.310}$ MPa, $\sigma_y = 200$ MPa, $r_{cf} = 50$ mm, $r_d = 8.5t_0$, $t_0 = 1$ mm) Experiment were carried out by Whiteley [1960].

conditions and different die geometry used in the experiments.

Table 4.1 shows the comparison between the predictions of the model developed by Sonis[2001] with the experimental results of Whiteley[1960] for mild steel. It can be seen that they are in good agreement. The data regarding the material properties, die geometry and lubricant used are not given by Whiteley [1960]. Therefore limiting drawing ratios are estimated

Material type	t_0 (mm)	K (Kpmm ⁻²)	σ_y (Kpmm ⁻²)	\bar{R}	n	LDR (Present)	LDR (exp.)	Δ LDR
HH Al	0.70	13.37	10.36	0.49	0.041	1.794	2.100	-0.306
Soft Al	0.70	12.02	2.93	0.61	0.227	1.968	2.053	-0.085
Soft 70/30 brass	0.75	75.30	3.69	0.83	0.485	2.271	2.190	+0.081

Table 4.2: Comparison of experimental and theoretical data of LDR for non ferrous sheets. Lubricant : Droyt-Sol 4M, mineral oil. $\mu = 0.10$, $r_{cf} = 19.6225$ mm, $r_d = 7.450$ mm. Experiment was carried out by El-Sebaie and Mellor [1972].

using the material properties of SAE 1006. Final cup radius and initial blank thickness are taken as 50mm and 1mm respectively. The discrepancy in the predictions can be attributed to the possible variations in the material properties, friction conditions and die geometry used in the experiments of Whiteley [1960].

Table 4.2 shows the comparison between the predictions of the model presented by Sonis[2001] with the experimental results of El-Sebaie and Mellor[1972]. They carried out experiments by forming the cylindrical cups from the circular blanks of nominal blank thickness of 0.71 mm. Punch head used had a stem diameter of 38 mm and a profile radius of 4 mm. The diameter of the die opening was 39.945 mm giving a radial clearance of 37% of nominal blank thickness. The blanks were lubricated on both sides using Droyt-Sol 4 M. A series of blanks were produced increasing in steps of 1 mm on the diameter. In the final stages of the tests to determine the limiting drawing ratio the increment of 1 mm was reduced to 0.4 mm. The conditions used by El-Sebaie and Mellor [1972] are used to estimate the limiting drawing ratio from the model presented by Sonis[2001]. For the lubricant Droyt-Sol 4 M, coefficient of friction (μ) is taken as 0.10 as reported by Leu[1999]. It can be seen that the results obtained are in good agreement with the results of El-Sebaie and Mellor [1972]. The discrepancy can be attributed to the bending and unbending of the sheet metal undergone during deep drawing, which is neglected in the present work. Also, the discrepancy can be attributed to static friction condition i.e., coefficient of friction will remain constant during the process, which is assumed in the analysis model developed by Sonis[2001].

Redraw

To establish the validity of the model presented by Sonis[2001], its predictions are compared with the suggested drawing ratios given in Handbook of Metal Forming, Lange[1985] for SAE 1006 and are shown in Table 4.3. Lange[1985] reported drawing ratios for deep drawing of cylindrical components with flat bottom for the different relative sheet thickness ranges (1.5-

Relative Sheet Thickness ($\frac{t_0}{D_0} \times 100$)						
Number of draws	Lange[1985]			Present Work		
	0.3-0.6	0.15-0.3	0.08-0.15	0.50	0.25	0.15
1	1.72-1.82	1.67-1.72	1.59-1.67	2.1	2.0	2.08
2	1.26-1.28	1.25-1.26	1.22-1.25	1.31	1.22	1.18
3	1.23-1.25	1.22-1.23	1.19-1.22	1.3	1.21	1.17
4	1.20-1.22	1.18-1.20	1.16-1.18	1.11	1.12	1.15
5	1.16-1.18	1.15-1.16	1.14-1.15	1.11	1.12	1.15

Table 4.3: Comparison of theoretical data of LDR for Redraws without intermediate annealing with Lange[1985] suggested drawing ratio. Sheet metal thickness, $t_0 = 1.0$ mm. *Source: Handbook of Blanking Technology, Romanowski[1959]*

2.0, 1.0-1.5, 0.6-1.0, 0.3-0.6, 0.15-0.3 and 0.08-0.15). The relative sheet thickness is given by

$$\frac{t_0}{D_0} \times 100$$

The relative sheet thickness is used to predict the severity of wrinkling (see Appendix B). For the relative sheet thickness less than 0.50, blank holder force is required to avoid wrinkling [Eary and Reed, 1974]. Present analysis has been carried out by considering the blank-holding force during deep drawing. Therefore comparisons are made for different relative sheet thickness values less than 0.50. The value of normal anisotropy for most of the deep drawing quality steels vary from 1.2 to 1.6 [ASM Handbook, 1992]. Here, for estimating the limiting drawing ratio, the value of normal anisotropy is taken as 1.4 for SAE 1006. The material properties of SAE 1006 steel are [ASM Handbook, 1992] given by

$$\text{Generalized stress } (\bar{\sigma}) = 617(\bar{\epsilon})^{0.310} \text{ MPa}$$

$$\text{Yield Strength } (\sigma_y) = 200 \text{ MPa}$$

$$\text{Normal Anisotropy } (\bar{R}) = 1.4$$

The thickness of the initial blank is chosen as 1.0 mm and the initial blank diameter is calculated to satisfy the chosen relative sheet thickness value. Since the data regarding the die geometry and friction condition are not reported by Lange[1985], die arc radius for the first draw is chosen as $8.5t_0$ and for the subsequent draws it is taken as 0.8 times of previous draw die arc radius [Lange, 1985] and coefficient of friction (μ) is taken as 0.10 [Schuler, 1998].

From the table 4.3, it can be seen that the predictions of the model presented by So-

Material type	t_0 (mm)	K (MPa)	σ_y (MPa)	\bar{R}	n	LDR_0 (1)	LDR_0 (2)	LDR_1 (1)	LDR_1 (2)
SAE 1006	1.0	617	200	1.4	0.31	2.11	2.0	1.25	1.3
DQ Killed	1.0	610	172	1.6	0.22	2.04	2.1	1.25	1.3
DQ rimmed	1.0	619	207	1.2	0.21	1.90	2.0	1.25	1.35

Table 4.4: Comparison between the predictions of the model presented by *Sonis*¹ [2001] and limiting drawing ratios suggested by www.ici.net/cust-pages/hardro.html², [1996]. SAE 1006($\bar{\sigma}_e = 617(\bar{\epsilon}_e)^{0.310}$ MPa, $\sigma_y = 200$ MPa), DQ Killed($\bar{\sigma}_e = 610(\bar{\epsilon}_e)^{0.22}$ MPa, $\sigma_y = 172$ MPa), DQ Rimmed($\bar{\sigma}_e = 619(\bar{\epsilon}_e)^{0.21}$ MPa, $\sigma_y = 207$ MPa), $r_{cf} = 50$ mm, $r_d = 8.5 * t_0$, $t_0 = 1$ mm

nis [2001] are in good agreement with the suggested drawing ratios of Lange [1985]. The discrepancy in the result may be due to the following reasons:

- different friction conditions used.
- different die geometry used.
- thickness of the sheet considered as 1.0 mm in the present work.
- bending and unbending effects which are neglected in the present work.

Table 4.4 shows the comparison between the predictions of the model presented by *Sonis* [2001] with the limiting drawing ratios suggested by www.ici.net/cust-pages/hardro/hardro.html [1996]. It can be seen that they are in good agreement. The data regarding die geometry and lubricant used are not given by him. Die design guidelines concerned to punch corner radius are taken from the section 2.3. In the present case, cup radius and initial blank thickness is taken as 50mm and 1mm respectively. The discrepancy in the predictions can be attributed to the possible variations in the friction conditions and die geometry used.

4.3 Case Studies

In the present work, four cases are considered to demonstrate the capabilities of the developed system. The components chosen for study do not contain flange portion and the last draw in the process plan table gives the final draw in which limiting drawing ratio is adjusted to get the required cup radius. For the case studies, the material is chosen is CA-DDQ steel, which has the maximum drawing ratio of approximately 6.5 [Lange, 1985]. When the material reaches this limit, it has to be annealed to achieve further reduction. In the present system, to be on the conservative side, its value is taken as 6.0.

4.3.1 Input Parameters to the System

This section presents the input parameters required by the system. They are as follows:

- Final Part Geometry (modeled using feature primitives): The final part geometry is required to determine the initial blank diameter using the Pappus's Second Theorem [section 2.2] with the trim allowance added to it.
- The cup thickness (t_0).
- Material properties, friction coefficient etc. from the system database.
- Runtime decisions from user for alternative process plans.

4.3.2 Output from the System

Given the input, the following output can be generated from the system.

- Material selected: The system displays the material chosen by the user [section 2.4].
- Suggested lubricant: According to the material selected by the user, the system suggests the lubricant to be used [Section 2.4].
- Press suggested: According to the calculated drawing force required, the system suggests the press to be used [Section 2.4].
- Blank radius: The blank radius is calculated using Pappus's second theorem with trim allowance added to it [Section 2.2].
- Die arc radius (r_d): The present system uses the die arc radius as 8.5 times the sheet thickness for the first draw and for subsequent redraws it is taken as 0.8 times the previous draw die arc radius [Section 2.3].
- Punch corner radius(r_p): In the present system, the punch corner radius for all draws is taken as 3 mm larger than the final punch corner radius (r_{pf}) and for the final draw it is equal to the required dimensions on the product [Section 2.3].
- Die-to-punch clearance: The system uses punch-to-die clearance as $1.09 t_0$ for the first draw, $1.10 t_0$ for redraws and $1.09 t_0$ for the final draw [Section 2.3].
- Limiting drawing ratio (LDR): Analysis model developed by Sonis [2001] is used to calculate the limiting drawing ratios for the first and subsequent draws [Section 2.4].
- Number of draws: The limiting drawing ratio in each pass decides the number of draws required to achieve the required drawing ratio.

- Annealing stage: If the material exceeds its maximum drawing ratio limit, it has to be annealed to achieve further deformation. The system suggests the stage at which annealing is required. There is a provision to select the annealing stage to generate all feasible process sequences.
- Percentage reduction: The percentage reduction at each draw is given by

$$\text{Percentage Reduction for first draw} = \left(\frac{R_0 - r_{c0}}{R_0} \right) \times 100$$

$$\text{Percentage Reduction for redraws} = \left(\frac{r_{c_{i-1}} - r_{c_i}}{r_{c_{i-1}}} \right) \times 100$$

where, $i = 1, 2, 3, \dots, N$.

4.3.3 Case I

To demonstrate the capabilities of the system developed, an example is selected which requires less reduction and the final shape can be achieved in one pass, without reaching the annealing limit. Table 4.5 shows the system output for this case. System output is presented below:

Input to the system:

Cup radius (r_{cf}) = 50 mm
Punch radius (r_{pf}) = 6.0 mm
Flange width (F_w) = 0.0
Final cup height (H) = 80 mm
Blank thickness (t_0) = 1.0 mm
Material = CA DDQ steel ($(\bar{\sigma}) = 610(\bar{\epsilon})^{0.263}$ MPa)

Output from the system:

Material = CA DDQ steel ($(\bar{\sigma}) = 610(\bar{\epsilon})^{0.263}$ MPa)
Lubricant suggested: Emulsified mineral oil ($\mu = 0.1$)
Press suggested: Single action hydraulic press
Initial blank radius (R_0) = 104.0 mm
Punch corner radius for draw "1" = 6 mm

4.3.4 Case II

Here, an example is selected in such a way that it requires two passes to achieve the cup radius. From the table 4.6 it is clear that the desired diameter reduction is achieved in two passes and the part does not require intermediate annealing.

No. of Draws (i)	Die Arc Radius r_d (mm)	Punch-to- die clearance (mm)	LDR_i	DR_{total}	Cup Radius $r_{c_{i-1}}$ (mm)	Percentage Reduction
1	8.5	1.09	2.08	2.08	50	51.9

Table 4.5: Process plan output (Case I)

Input to the system:

Cup radius (r_{c_f}) = 50.0 mm

Punch radius (r_{p_f}) = 6.0 mm

Flange width (F_w) = 0.0

Final cup height (H) = 190 mm

Blank thickness (t_0) = 1.0 mm

Material = CA DDQ steel ($(\bar{\sigma}) = 610(\bar{\epsilon})^{0.263}$ MPa)

Output from the system:

Material = CA DDQ steel ($(\bar{\sigma}) = 610(\bar{\epsilon})^{0.263}$ MPa)

Lubricant suggested: Emulsified mineral oil ($\mu = 0.1$)

Press suggested: Single action hydraulic press

Initial blank radius (R_0) = 150.0 mm

Punch corner radius for draw "1" = 9 mm

Punch corner radius for draw "2" = 6 mm

No. of Draws (i)	Die Arc Radius r_d (mm)	Punch-to- die clearance (mm)	LDR_i	DR_{total}	Cup Radius $r_{c_{i-1}}$ (mm)	Percentage Reduction
1	8.5	1.09	2.31	2.31	65	56.7
2	6.8	1.09	1.3	3.07	50.0	23.1

Table 4.6: Process plan output (Case II)

4.3.5 Case III

From the table 4.7 it is clear that the desired diameter reduction is achieved in three passes and the part does not require intermediate annealing.

Input to the system:

Cup radius (r_{cf}) = 50.0 mm

Punch radius (r_{pf}) = 5.0 mm

Flange width (F_w) = 0.0 mm

Final cup height (H) = 280 mm

Blank thickness (t_0) = 1.0 mm

Material = CA DDQ steel ($(\bar{\sigma}) = 610(\bar{\epsilon})^{0.263}$ MPa)

Output from the system:

Material = CA DDQ steel ($(\bar{\sigma}) = 610(\bar{\epsilon})^{0.263}$ MPa)

Lubricant suggested: Emulsified mineral oil ($\mu = 0.1$)

Press suggested: Single action hydraulic press

Initial blank radius (R_0) = 179.0 mm

Punch corner radius for draws "1-2" = 8.0 mm

Punch corner radius for draw "3" = 5.0 mm

No. of Draws (i)	Die Arc Radius r_d (mm)	Punch-to- Die Clearance (mm)	LDR_i	DR_{total}	Cup Radius r_{ci-1} (mm)	Percentage Reduction
1	8.5	1.09	2.29	2.29	78.1	56.4
2	6.8	1.10	1.27	2.9	61.71	20.98
3	5.4	1.09	1.23	3.56	50	18.98

Table 4.7: Process plan output without annealing (Case III)

In this case, even though the annealing stage has not reached, if the annealing is performed after the first draw, the process sequence would consist of two draws only. The limiting drawing ratio obtained after annealing is 2.41. In order to achieve the required cup radius, the limiting drawing ratio is adjusted in the final draw as shown in Table 4.8. It depends on the process planner to select the process plan which has the least production cost by considering the annealing and tooling costs. Cost comparisons are not considered in the present work.

No. of Draws (<i>i</i>)	Die Arc radius r_d (mm)	Punch-to- die clearance (mm)	LDR_i	DR_{total}	Cup Radius $r_{c_{i-1}}$ (mm)	Percentage Reduction
1	8.5	1.09	2.29	2.29	78.1	56.4
2*	6.8	1.09	1.56	1.56	50	35.89

Table 4.8: Process plan output with annealing after first draw (Case III)

4.3.6 Case IV

In this case, the part is selected such that the total drawing ratio exceeds the critical drawing ratio of the material selected that can be achieved without intermediate annealing.

Input to the system:

Cup radius (r_{cf}) = 50.0 mm

Punch radius (r_{pf}) = 4.0 mm

Flange width (F_w) = 0.0 mm

Final cup height (H) = 1330 mm

Blank thickness (t_0) = 1.0 mm

Material = CADDQ steel ($(\bar{\sigma}) = 610(\bar{\epsilon})^{0.263}$)

Output from the system:

Material = CA DDQ steel ($(\bar{\sigma}) = 610(\bar{\epsilon})^{0.263}$)

Lubricant suggested: Emulsified mineral oil ($\mu = 0.1$)

Press suggested: Single action hydraulic press

Initial blank radius (R_0) = 380 mm

Punch corner radius for all draws (except final draw) = 7 mm

Punch corner radius for final draw = 4 mm

In this case, the required cup radius cannot be achieved without annealing as the critical drawing ratio is exceeded in the seventh pass [table 4.9]. Thus annealing is required after sixth pass. As annealing is necessary to achieve the required cup radius. Tables 4.10 to 4.12 shows the alternative process plans generated by the system (after taking the input from the user regarding the annealing stage) when annealing is done after first, second and third draw.

No. of Draws (i)	Die Arc Radius r_d (mm)	Punch-to-die clearance (mm)	LDR_i	DR_{total}	Cup Radius $r_{c_{i-1}}$ (mm)	Percentage Reduction
1	8.5	1.09	2.25	2.25	168.98	55.52
2	6.8	1.10	1.20	2.69	140.6	16.67
3	5.4	1.10	1.20	3.22	117.3	16.67
4	4.4	1.10	1.187	3.82	98.95	15.75
5	4.4	1.10	1.187	4.53	83.36	15.75
6	4.4	1.10	1.187	5.38	70.23	15.75
7	4.4	1.10	1.177	6.33	59.66	15.0

Table 4.9: Process plan output without Annealing($t_0 = 1.0$ mm)

No. of Draws (i)	Die Arc Radius r_d (mm)	Punch-to-die clearance (mm)	LDR_i	DR_{total}	Cup Radius $r_{c_{i-1}}$ (mm)	Percentage Reduction
1	8.5	1.09	2.25	2.25	168.89	55.52
2*	6.8	1.10	2.29	2.29	73.58	56.45
3	5.4	1.10	1.25	2.87	58.86	20.0
4	4.4	1.09	1.18	3.37	50.0	15.05

Table 4.10: Annealing after first draw

From tables 4.10 and 4.11 it is clear that the number of stages required to achieve the required reduction are same. If the annealing is performed after the third stage, the number of pass required [table 4.12] to achieve the required reduction are higher than that of when annealing is performed after first and second draw [tables 4.10 and 4.11]. The strength of the cup, however, would be more when annealing is performed after first draw since strain induced in this case would be more. Hence, the process sequence for the given part should have annealing stage after the first draw. The selected process plan is shown in the Table 4.13

No. of Draws (i)	Die Arc Radius r_d (mm)	Punch-to-die clearance (mm)	LDR_i	DR_{total}	Cup Radius $r_{c_{i-1}}$ (mm)	Percentage Reduction
1	8.5	1.09	2.25	2.25	168.89	55.5
2	6.8	1.10	1.20	2.69	140.6	16.67
3*	5.4	1.10	2.29	2.29	61.6	56.3
4	4.4	1.09	1.23	2.82	50.0	18.69

Table 4.11: Annealing after second draw

No. of Draws (i)	Die Arc Radius r_d (mm)	Punch-to-die clearance (mm)	LDR_i	DR_{total}	Cup Radius $r_{c_{i-1}}$ (mm)	Percentage Reduction
1	8.5	1.09	2.25	2.25	168.89	55.5
2	6.8	1.10	1.20	2.69	140.6	16.67
3	5.4	1.10	1.20	3.22	117.3	16.67
4*	4.4	1.10	2.29	2.29	51.48	56.34
5	3.5	1.09	1.03	2.35	50.0	3.1

Table 4.12: Annealing after third draw

No. of Draws (i)	Die Arc Radius r_d (mm)	Punch-to-die clearance (mm)	LDR_i	DR_{total}	Cup Radius $r_{c_{i-1}}$ (mm)	Percentage Reduction
1	8.5	1.09	2.25	2.25	169	55.5
2*	6.8	1.10	2.25	2.25	75.1	55.5
3	5.4	1.10	1.27	2.86	59	21.5
4	4.4	1.09	1.18	3.65	50.0	15.3

Table 4.13: Process plan output (Case IV)

Tables 4.14 shows that the limiting drawing ratio increases with the increase in the sheet thickness (when blank thickness is increased from 1.0 mm to 1.5 mm). Thus with increase in the blank thickness, the total drawing ratio exceeds the critical drawing ratio in less number of passes.

No. of Draws (i)	Die Arc Radius r_d (mm)	Punch-to-die clearance (mm)	LDR_i	DR_{total}	Cup Radius $r_{c_{i-1}}$ (mm)	Percentage Reduction
1	12.75	1.63	3.11	3.11	121.98	67.89
2	10.2	1.65	1.5	4.67	81.32	33.33
3	8.16	1.65	1.43	6.717	56.57	30.43

Table 4.14: Process plan output without Annealing($t_0 = 1.5$ mm)

In this case, the required cup radius cannot be achieved without annealing as the critical drawing ratio is exceeded in the third pass [table 4.14]. Thus annealing is required after second pass. Tables 4.15 and 4.16 shows the alternative process plans generated by the system (after taking the input from the user regarding the annealing stage) when annealing is done after first and second draw.

No. of Draws (i)	Die Arc Radius r_d (mm)	Punch-to-die clearance (mm)	LDR_i	DR_{total}	Cup Radius $r_{c_{i-1}}$ (mm)	Percentage Reduction
1	12.75	1.63	3.11	3.11	121.98	67.89
2*	10.2	1.63	2.44	2.44	50	59.01

Table 4.15: Annealing after first draw ($t_0 = 1.5$ mm)

From tables 4.15 and 4.16 it is clear that the annealing is performed after first stage, the number of pass required [table 4.15] to achieve the required reduction are lesser than that of when annealing is performed after second draw [tables 4.16. Hence, the process sequence for the given part (with blank thickness = 1.5 mm) should have annealing stage after the first draw.

No. of Draws (i)	Die Arc Radius r_d (mm)	Punch-to- die clearance (mm)	LDR_i	DR_{total}	Cup Radius $r_{c_{i-1}}$ (mm)	Percentage Reduction
1	12.75	1.63	3.11	3.11	121.98	67.89
2	10.2	1.65	1.5	4.672	81.32	33.33
3*	8.16	1.63	1.62	1.62	50	38.51

Table 4.16: Annealing after second draw ($t_0 = 1.5$ mm)

4.4 Journey Through the System

In this case, the working of the system is demonstrated to achieve the alternate process plans. The system involves the following steps to achieve the final result as shown from Figure 4.3 to 4.9.

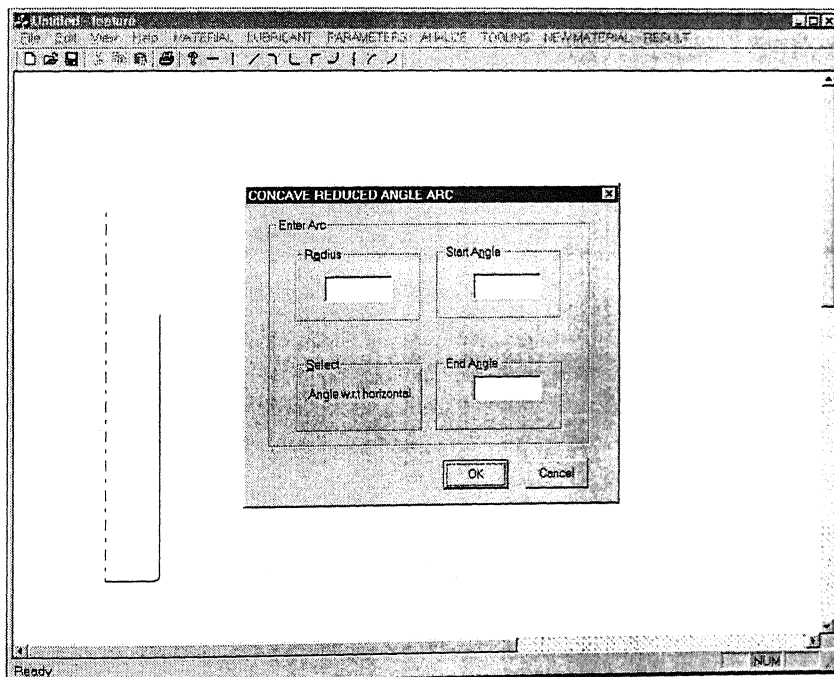


Figure 4.3: Object modelling using geometric primitives

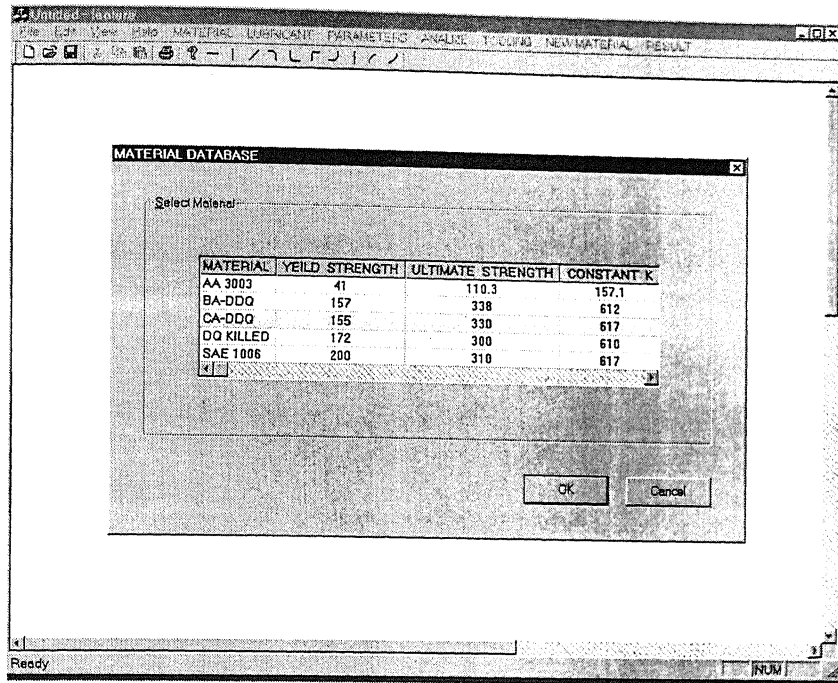


Figure 4.4: Material selection

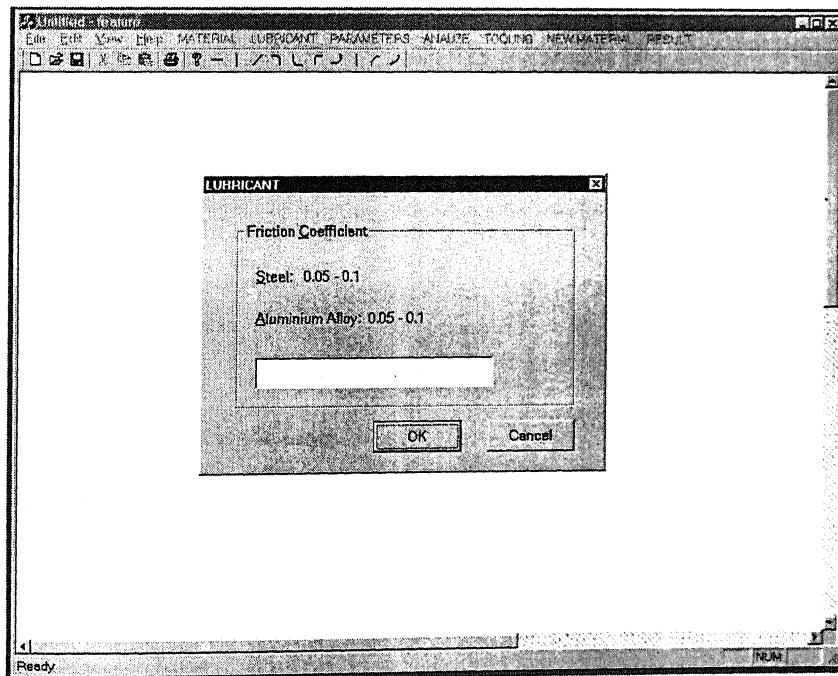


Figure 4.5: Lubricant selection

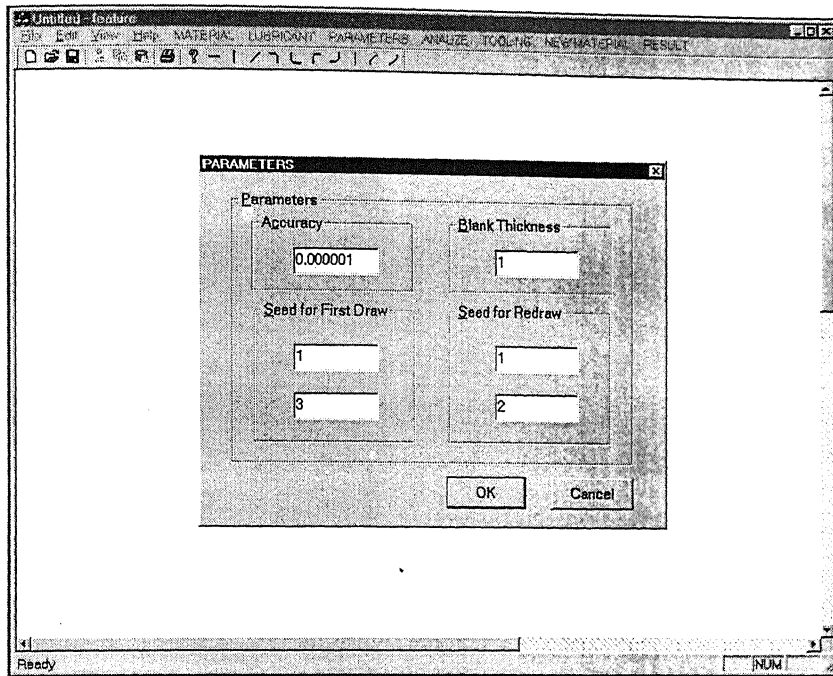


Figure 4.6: Operating parameters

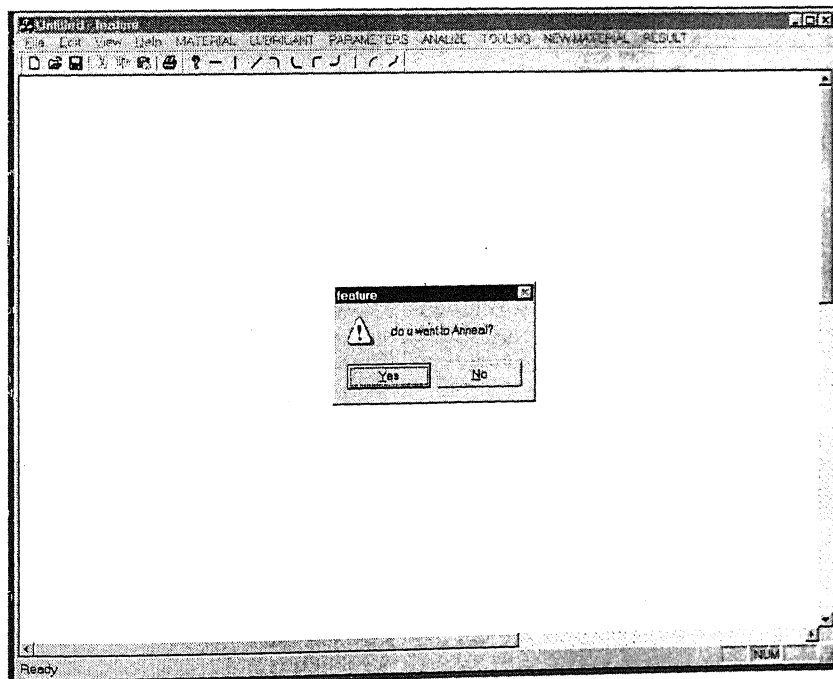


Figure 4.7: Realtime decision for annealing

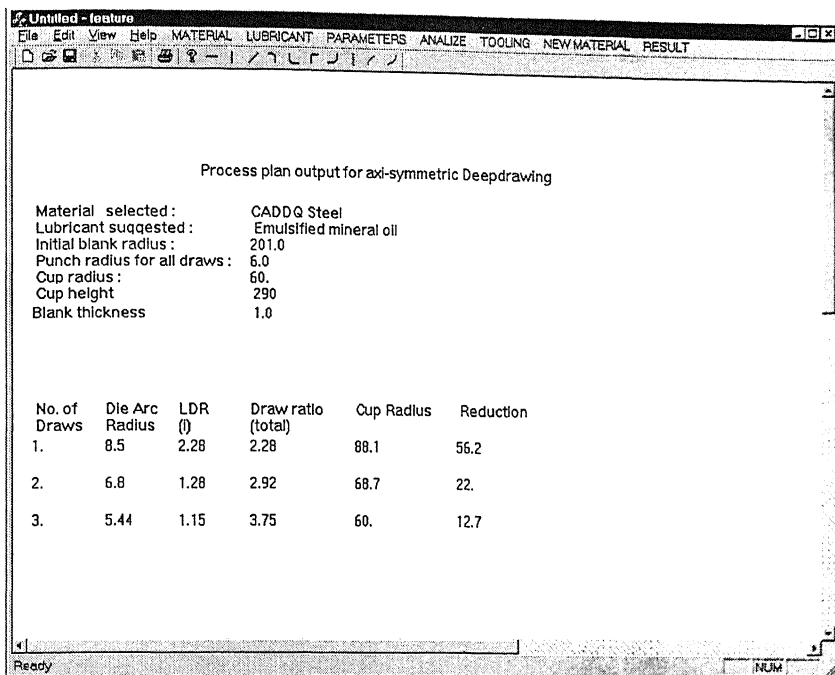


Figure 4.8: Process plan without annealing

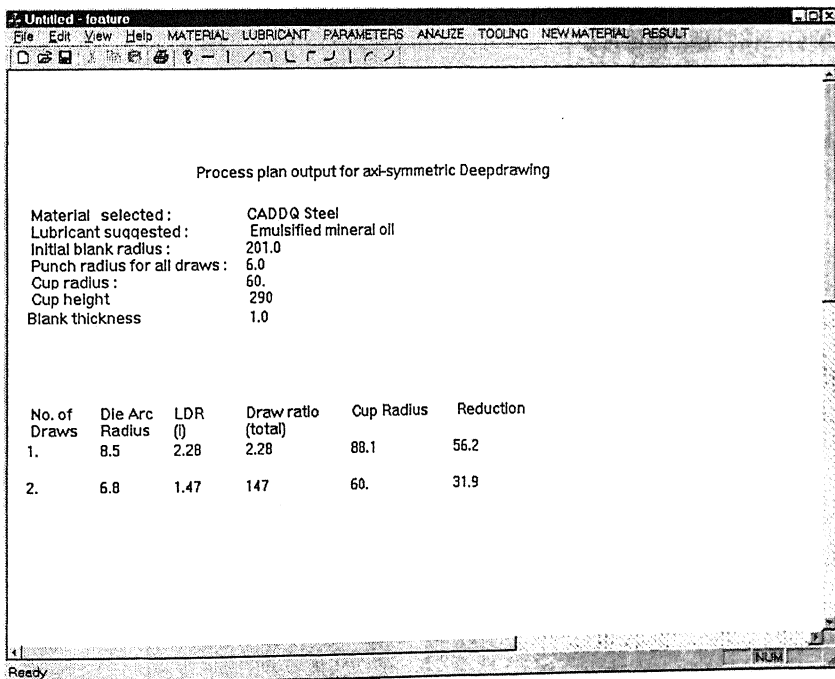


Figure 4.9: Process plan with annealing

Chapter 5

Conclusions and Scope for the Future Work

5.1 Conclusions

The following conclusions are drawn from the present work:

- An attempt is made to develop an intelligent aid to the process planner of deep drawing components.
- Parametric product design module is developed.
- The model presented by Sonis[2001] is based on the force equilibrium method can predict the limiting drawing ratio close to the experimental results for the first draw [Whiteley, 1960 ; Rogers and Anderson, 1971 and El-Sebaie and Mellor, 1972]. Also, the limiting drawing ratio predicted are in good agreement with the limiting drawing ratios available in standard metal forming handbook [Lange, 1985].
- The database of the system designed to be flexible with an easily extendable structure. Database can be modified with recompiling the system module for effective database management.
- The proposed model has been implemented to generate process plan for manufacturing of axisymmetric deep drawing components. From the case study, it is clear that by selecting the appropriate annealing stage, the total number of draws required to achieve the desired cup geometry can be reduced.
- The knowledge based system developed generates all feasible process plans considering formability limits and the rules in the database, user can select the best among them.
- The computational time taken to generate the process plan is very low.

5.2 Scope for the Future Work

Further work can be carried out in the following aspects for process planning of deep drawing components:

- Three dimensional volumetric modeling can be done for the geometric description.
- In the present work, bending and unbending of the sheet metal during deep drawing is not considered and they have to be included to get more accurate results.
- Optimal geometrical sequencing in conjunction with the analysis model can be generated.
- Data can be collected from industries and added to the database.

References

Ahmetoglu, M., Broek, T.R., Kinzel, G., Altan, T., Control of Blank Holder Force to Eliminate Wrinkling and Fracture in Deep Drawing Rectangular Parts, *Annals of CIRP*, Vol. 44, No. 1, pp 247-250, 1995.

Altan, T, Oh, S.I., and Gegel, H., *Metal Forming: Fundamentals and Applications*, ASM Internatioanl, 1983.

Atkinson, M., *Sheet Metal Industries*, Vol. 44, pp 167-178, 1967.

Chiang, D.C., and Kobayashi, Shiro, The Effect of Anisotropy and Workhardening Characteristics on Stress and Strain Distribution in Deep Drawing, *Trans ASME, Journal for Engg. for Industry*, Nov. 1966.

Chung, S.Y. and Swift, H.W., Cup Drawing from a Flat Blank. Part I Experimental Investigation, *Proc. Instn Mech. Engrs.*, U.K. pp 199-211, 1951.

ASM Handbook, 1992.

Doege, E., Schulte, S. Design of Deep Drawn Components with Elementary Calculation Methods, *J. of Mat. Processing Tech.*, Vol.34, pp 439 -447, 1992.

Die Design HandBook, McGraw-Hill Book Co. Inc.,1955.

Eary, D.F., and Reed, E.A., *Techniques of pressworking sheet metal*, Prentice Hall, Englewood Cliffs.

Emani, S. Axisymmetrical Plastic Flow of Anisotropic Sheet During Deep Drawing, *Sheet Metal Industries*, No. 4, April 1984.

El-Sebaie and Mellor, P.B., Plastic Instability Conditions in the Deep Drawing of a Circular Blank of Sheet Metal, *Int. J. of Mech. Science*, Vol. 14, pp 535-556, 1972.

Esche. S.K., Khamitkar, S., Kinzel, G.L., Altan T., Process and Die Design for Multi-step Forming of Round Parts from Sheet Metal, *J. of Mat. Processing Tech.*, Vol. 59, pp 24-33, 1996.

Esche, S.K., Ahmetoglu, M., Kinzel, G.L., Altan T., Numerical and Experimental Investigation of Redrawing of Sheet Metals, *J. of Mat. Processing Tech.*, Vol. 98, pp 17-24, 2000.

Eshel, G., Barash, M. and Johnson, W., Rule Based Modeling for Planning Axisymmetrical Deep Drawing, *J. of Mech. Working Tech.*, Vol.14, pp 1-115, 1986.

Fogg, B., Theoretical Analysis for the Redrawing of the Cylindrical Cups Through Conical Dies Without Pressure Sleeves, *J. of Mech. Engrs Science*, Vol. 10, pp 141-152, 1968.

Ghosh, A. and Mallik, A.K., *Manufacturing Science*, Affiliated East-West Press Publishers Ltd., 1994.

Haleri, G., and Weil, R.D., *Principle of Process Planning*, Chapman and Hall, 1995.

Hill, R., *The Mathematical Theory of Plasticity*, Clarendon Press, Oxford (U.K.), 1950.

Hosford, W.F., and Caddell, R.M., *Metal Forming - Mechanics and Metallurgy*, Prentice Hall, Englewood Cliffs, 1983

Johnson, W., and Mellor, P.B., *Engineering Plasticity*, Van Nostrand and Reinhold, 1972.

Korhonen, A.S., Drawing Force in Deep Drawing of Cylindrical Cup with Flat Nosed Punch, *J. for Engg. for Ind.*, Vol 104, pp 29-37, 1982.

Lange, K., *HandBook of Metal Forming*, McGraw-Hill Book Co., 1985.

Leu, D.K., Prediction of the Limiting Drawing Ratio and the Maximum Drawing Load in Cup Drawing, *Int. J. of Mach. Tools Manuf.*, Vol. 37, No. 2, pp 201-213, 1997.

Leu, D.K., The Limiting Drawing Ratio for Plastic Instability of the Cup Drawing Process *Int. J. of Mat. Processing Tech.*, Vol. 86, No. 2, pp 168-176, 1999.

Miller, F.H., *Analytical Geometry and Calculus*, Chapman and Hall Ltd., 1949.

Min, D.K., Jeon, B.H., Kim, H.J., Kim, N., A Study on Process Improvements of Multi-Stage Deep Drawing by The Finite Element Method, *Int. J. of Mat. Processing Tech.*, Vol. 54, pp 230-238, 1995.

Oskada, K., Wang, C.C. and Mori, K. Controlled FEM Simulation for Determining History of Blank Holding Force in Deep Drawing, *Annals of CIRP*, Vol. 44, No. 1, pp 243-246, 1995.

Parsa, M.H., Yamaguchi, K., Takakura, N., Imatani, S., Consideration of the Redrawing of Sheet Metals Based on Finite Element Simulation, *Int. J. of Mat. Processing Tech.*, Vol. 47, pp 87-101, 1994.

Rao, I.V., A Parameter Optimization Module for CAPP for Multi-Stage Deep Drawing, *M.Tech. Thesis, I.I.T. Kanpur*, 1998.

Reissner, J., and Meier, M., Instability of the Annular Ring as a Deep Drawn Flange Under Real Conditions, *Annals of CIRP*, Vol. 32, No.1, pp 187-190, 1983.

Reissner, J., and Ehrismann, R., Computer-Aided Deep Drawing of Two Part Cans, *Annals of CIRP*, Vol. 36, pp 199-202, 1987.

Rogers, R.W., and Anderson, W.A., Effect of Plastic Anisotropy on Drawing characteristics of Aluminium Alloy sheet, *Metal Forming-Interrelation between theory and practice*, Edited by A.L. Hoffmanner, 1971, Plenum Press, New York, London.

Sachs, G. *Principles and Methods of Sheet-Metal Fabricating*, Reinhold Publishing Corporation, 1960.

Sitaram, S.K., Kinzel, G.L., and Altan T., A Knowledge Based System for Process Sequence Design in Axisymmetric Sheet Metal Forming, *J. of Mat. Processing Tech.*, Vol.25, pp 247 -271, 1991.

Schuler, *Metal Forming HandBook*, Springer, 1998.

Suzuki, K., The Relationship Between the Deep Drawability and the r-values of Sheet Metals, *J. of Mech. Working Tech.*, Vol.15, pp 131-142, 1987.

Siegert, K., Dannenmann, E., Wagner, S. and Galaiko A., Closed Loop Control System For Blank Holder Forces in Deep Drawing *Annals of CIRP*, Vol. 44, No. 1, pp 251-254, 1995.

Sonis, Process Analysis and Computer-Aided Process Planning for Deep Drawing of Axisymmetric Components, *M-Tech Thesis*, 2001.

Tisza, M. Expert Systems for Metal Forming, *J. of Mat. Processing Tech.*, Vol. 53, pp 423 -432, 1995.

Toh, K.H.S., Loh, H.T. Nee, A.Y.C. and Lee, K.S. A Feature Based Flat Development System for Sheet Metal Parts. *J. of Mat. Processing Tech*, Vol. 48, pp 89-95, 1995

Wallace, J.W., Improvement In Punches For Cylindrical Deep Drawing, *Sheet Metal Industries*, pp 901-904, Dec 1960.

Wilson, D.V., Sunter, B.J., and Martin D.F., *Sheet Metal Industries*, Vol. 43, pp 465-476, 1966.

Wright J.C., Relationship Between Mechanical Properties, Deep Drawability and Stretch-Formability for some non-ferrous Sheet Materials, *Sheet Metal Industries*, pp 887-901, Dec 1962.

Woo, D.M., On The Complete Solution The Deep Drawing Problem, *Int. J. of Mech. Science*, Vol. 10, 1968.

Yu, T.X. and Johnson, W., The Buckling of Annular Plates in Relation to the Deep Drawing Process, *Int. J. of Mech. Science*, Vol. 24, No. 3, pp 175-188, 1982.

Appendix A: Solutions of the Integral Terms

I

$$\begin{aligned}
 \int_{r_{cd}}^{r_0} \left(\ln \frac{R}{r} \right)^n \frac{dr}{r} &= \int_{r_{cd}}^{r_0} \left[1 + \left(\ln \frac{R}{r} - 1 \right) \right]^n \frac{dr}{r} \\
 &= \int_{r_{cd}}^{r_0} \left[1 + n \left(\ln \frac{R}{r} - 1 \right) \right] \frac{dr}{r} \\
 &= n \int_{r_{cd}}^{r_0} \ln \frac{R}{r} \frac{dr}{r} + (1 - n) \ln \frac{r_0}{r_{cd}}
 \end{aligned} \tag{5.1}$$

The integral term at the right side of the Eq. () can also be approximated as :

$$\begin{aligned}
 \int_{r_{cd}}^{r_0} \ln \frac{R}{r} \frac{dr}{r} &= \int_{r_{cd}}^{r_0} 2 \left[\frac{\frac{R}{r} - 1}{\frac{R}{r} + 1} \right] \frac{dr}{r} = 2 \int_{r_{cd}}^{r_0} \left(1 - \frac{2r}{R + r} \right) \frac{dr}{r} \\
 &= 2 \ln \frac{r_0}{r_{cd}} - 4 \int_{r_{cd}}^{r_0} \frac{1}{R + r} dr
 \end{aligned} \tag{5.2}$$

Based on the volume constancy of the plastic deformation in the flange region of the cup-drawing, i.e. $R_0^2 - r_0^2 = R^2 - r^2 = R_2^2 - r_{cd}^2 = C^2 = \text{constant}$, Eq. () can be expressed as

$$\begin{aligned}
 \int_{r_{cd}}^{r_0} \ln \frac{R}{r} \frac{dr}{r} &= 2 \ln \frac{r_0}{r_{cd}} - \frac{4}{C^2} \int_{r_{cd}}^{r_0} (R - r) dr \\
 &= 2 \ln \frac{r_0}{r_{cd}} - \frac{4}{C^2} \left(\int_{r_{cd}}^{r_0} \sqrt{C^2 + r^2} dr - \frac{r_0^2 - r_{cd}^2}{2} \right) \\
 &= 2 \left[\ln \frac{r_0}{r_{cd}} - \frac{1}{C^2} \left(R_0 r_0 - R_2 r_{cd} + C^2 \ln \frac{R_0 + r_0}{R_2 + r_{cd}} \right. \right. \\
 &\quad \left. \left. - r_0^2 + r_{cd}^2 \right) \right]
 \end{aligned} \tag{5.3}$$

Sustituting the above terms in Eq.(), the following equation., i.e. Eq. (0 can be obtained:

$$\int_{r_{cd}}^{r_0} \left(\ln \frac{R}{r} \right)^n \frac{dr}{r} = (1 + n) \ln \frac{r_0}{r_{cd}} - 2n \left(\ln \frac{R_0 + r_0}{R_2 + r_{cd}} + \frac{r_0}{R_0 + r_0} - \frac{r_{cd}}{R_2 + r_{cd}} \right) \tag{5.4}$$

II

$$\begin{aligned}
 \int_{r_{cd}}^{r_{c0}} \ln \frac{R}{r} \frac{dr}{r} &= \int_{r_{cd}}^{r_{c0}} 2 \left[\frac{\frac{R}{r} - 1}{\frac{R}{r} + 1} \right] \frac{dr}{r} = 2 \int_{r_{cd}}^{r_{c0}} \left(1 - \frac{2r}{R+r} \right) \frac{dr}{r} \\
 &= 2 \ln \frac{r_{c0}}{r_{cd}} - 4 \int_{r_{cd}}^{r_{c0}} \frac{1}{R+r} dr
 \end{aligned} \tag{5.5}$$

Let R_{i+1} be the intermediate radius on the base of the cup after I pass. From the volume constancy, $R^2 - r^2 = R_{i+1}^2 - r_{cd}^2 = C^2 = \text{constant}$

$$\begin{aligned}
 4 \int_{r_{cd}}^{r_{c0}} \frac{1}{R+r} dr &= 4 \int_{r_{cd}}^{r_{c0}} \frac{R-r}{C^2} dr \\
 &= \frac{4}{C^2} \int_{r_{cd}}^{r_{c0}} \sqrt{C^2 + r^2} dr - \int_{r_{cd}}^{r_{c0}} r dr \\
 &= \frac{2}{C^2} \left[\left(r \sqrt{C^2 + r^2} - C^2 \ln(r + \sqrt{C^2 + r^2}) \right) \Big|_{r_{cd}}^{r_{c0}} - (r_{c0}^2 - r_{cd}^2) \right] \\
 &= \frac{2}{C^2} \left[r_{c0} \sqrt{R_{i+1}^2 - r_{cd}^2 + r_{c0}^2} - r_{cd} R_{i+1} - (r_{c0}^2 - r_{cd}^2) - (R_{i+1}^2 - r_{cd}^2) \left[\ln \frac{r_{c0} + \sqrt{R_{i+1}^2 - r_{cd}^2 + r_{c0}^2}}{r_{cd} + R_{i+1}} \right] \right]
 \end{aligned}$$

Equation becomes

$$\begin{aligned}
 \int_{r_{cd}}^{r_{c0}} \ln \frac{R}{r} \frac{dr}{r} &= 2 \left[\ln \frac{r_{c0}}{r_{cd}} - \frac{1}{R_{i+1}^2 - r_{cd}^2} \left[r_{c0} \sqrt{R_{i+1}^2 - r_{cd}^2 + r_{c0}^2} - r_{cd} R_{i+1} - (r_{c0}^2 - r_{cd}^2) \right. \right. \\
 &\quad \left. \left. - (R_{i+1}^2 - r_{cd}^2) \left[\ln \frac{r_{c0} + \sqrt{R_{i+1}^2 - r_{cd}^2 + r_{c0}^2}}{r_{cd} + R_{i+1}} \right] \right] \right]
 \end{aligned} \tag{5.6}$$

137933

137933

Date Slip

The book is to be returned on
the date last stamped.

This image shows a blank sheet of white paper designed for handwriting practice. A solid black vertical line runs down the center of the page. On either side of this central line, there are ten horizontal rows of small black dots. These dots form a guide for letter height and placement. The entire sheet is framed by a thin black border at the top and bottom.